Thanks for submitting your manuscript to AMT. The manuscript is suitable for publication with technical revision. Please find below some technical comments that should be addressed in the final submission.

Dear Editor,

We sincerely appreciate the comments and suggestions from you. Thank you very much for considering the publication of our manuscript. We address your comments below (also in blue). The line number is corresponding to the change-tracked version.

Throughout the manuscript, when using trade names, please be sure to include the manufacturer and their place of business. For example, you do this for Igor Pro, but not for COMSOL, or for TSI, or for FC-43, or for Lindberg/Blue.

Response: we added the business place for COMSOL (line 255), TSI (line 15), FC-43 (line 79, the original paper didn't mention the business place for this chemical, thus, we included the reference), Lindberg/Blue (line 187).

Line 197: Use "vWCPC 3789" for consistency.

Response: revised in line 194.

Line 258: Use "vWCPC 3789" for consistency.

Response: revised in line 257. We revised the manuscript to use "vWCPC 3789"

Line 264: Change "decrease" to "decreased" (the rest of the paragraph is in past tense).

Response: changed to "decreased" in line 290.

Line 303: Change "condenser" to "conditioner"

Response: changed to "conditioner" in line 334.

Fig. 4. Please replot using a color scale that is more readable by those with color-vision impairment. Within Igor Pro, EOSSpectral11 is a good choice.

Response: we revised the color scale in Fig. 4. We used MATLAB for plotting and followed a color suggestion from a figure designer.

Fig. 5. For the color-vision impaired, pleas change one of the two filled circle symbols to a different shape (e.g., open circle or triangle). Same for the asterisk symbols.

Response: revised Fig. 5.

Fig. 5. Should there be two sets of dashed lines for each of the panels, showing the starting and ending points of the moderator?

Response: we added the additional dash lines in Fig. 5.

Line 356: Change "initator" to "initiator".

Response: changed to “initiator” in line 390.

Fig. 6 caption: Change "CPC 3789" to "vWCPC 3789".

Response: change in the caption.

I'm a bit confused at lines 374-375. "The reported pulse height. . . indicates the fraction of the particle population. . . ." I don't believe that pulse height indicates a fraction. Please restate more clearly. Further, "pulse height is above 90%. . .". 90% of what? Its nominal height? Same on line 378.

Response: Sorry for the confusion, we revised in line 414-416. “The reported “pulse height” by a vWCPC 3789 is not the pulse height value produced by the light scattering signal. It is a calculated parameter, which indicates the fraction of the particle population generating an acceptably high pulse. The manufacturer's manual states that the pulse height is above 0.9 for moderate concentrations (~10-5,000 cm^{-3}).”

The first paragraph in section 3.3 mixes up verb tenses, with "is" being used when referring to past measurements (e.g., line 379). Please use past tense ("was") consistently throughout this manuscript when referring to previously collected observations. However, when referring to a current analysis or interpretation of the data (e.g., line 385), still use "is". The last sentence should be, "When the pulse height was less than. . . ."

Response: we revised the section 3.3.

Figure 7. In panel a, please explain the units on the y-axis. This looks like normalized pulse height (relative to pulse height at 1000 hPa).

Response: see the above explanation for Fig. 7. We changed the y axis to “pulse height ratio”.

Line 425. What is meant by the "absorbing qualities" of humic acid? Are you saying that light absorption by humic acid has an effect? Or are you talking about absorption of water? Please specify what is meant.

Response: we revised it to “…light absorbing properties of humic acid” in line 474.

Fig. 8. Please use different symbol types for the different curves, and refer to the instrument as a "vWCPC 3789" in the caption.

Response: we revised Fig. 8.

Line 452. Pleas change to "For butanol-based CPCs such as the TSI 7610, the CPC. . . ."

Response: changed in line 519.

Line 456. Please change tense from "was" to "is".

Response: changed in line 522.

Line 446. Please change to "vWCPC 3789".

Response: changed 512.

Line 461. Change from "the AS particle" to "AS particles".

Response: changed in line 527.

Line 461. I don't understand why using a Vienna-style differential mobility analyzer affects the sharpness of the cut-point at surface pressure. If the DMA type is irrelevant, just say that that TSI response curve was determined at near-sea-level pressure; thus the curve is sharper.

Response: we revised it to "Note that the counting efficiency curve from TSI at 30 ℃ was derived and fitted using AS particle classified by a custom-made different mobility analyzer (using an aerosol to sheath flowrate ratio of 1:100) under a near-sea-level pressure" in line 526-528.

Fig. 9. Please use different symbols instead of just different colors. Change "CPC 3789" to "vWCPC3789".

Response: we revised Fig. 9 and changed the caption.

Line 486: Change in verb tense; change "is" to "was".

Response: changed in line 554.

Under "Competing interests", you may wish to state which authors have a commercial interest in the success of the vWCPC instrument.

Response: we revised the "competing interests".

Please thoroughly edit the references and ensure they meet Copernicus guidelines. Formatting is inconsistent. For example, sometimes article titles are capitalized; sometimes not. This is a result of reference manager-type software, which always messes up the formatting and needs to be checked by hand very thoroughly. It will save the Copernicus editorial staff considerable time if you go ahead and make these changes.

Response: Thank you very much for mentioning the software shortcoming. We revised the reference.

Supplemental material: I do not see a revised Supplemental Material file with tracked changes. Please provide one with tracked changes attached to the revised submission.

Response: The upload website didn't include the option to upload a change-tracked file for supplemental material, only for the main manuscript. Thus, we didn't upload one. We will combine it with the change-tracked main manuscript.

Simulation-aided characterization of a versatile water condensation particle counter for atmospheric airborne research

Fan Mei[1], Steven Spielman[2], Susanne Hering[2], Jian Wang[3], Mikhail Pekour[1], Gregory Lewis[2], Beat Schmid[1], Jason Tomlinson[1], Maynard Havlicek[4]

[1]Pacific Northwest National Laboratory, Richland, WA, 99352, USA
[2]Aerosol Dynamics Inc., Berkeley, CA, 94710, USA
[3]Washington University in St. Louis, St. Louis, MO, 63130, USA
[4]TSI Incorporated, Shoreview, MN, 55126, USA

Correspondence to: Fan Mei (fan.mei@pnnl.gov)

Abstract

Capturing the vertical profiles and horizontal variations of atmospheric aerosols often requires accurate airborne measurements. With the advantage of avoiding health and safety concerns related to the use of butanol or other chemicals, water-based condensation particle counters have emerged to provide measurements under various environments. However, airborne deployments are relatively rare due to the lack of instrument characterization under reduced pressure at flight altitudes. This study investigates the performance of a commercial "versatile" water CPC (vWCPC, Model 3789, TSI, Shoreview, MN, USA) under various ambient pressure conditions (500 – 920 hPa) with a wide range of particle total number concentrations (1,500 ~ 70,000 cm^{-3}). The effect of conditioner temperature on vWCPC 3789 performance at low pressure is examined through numerical simulation and laboratory experiments. We show that the default instrument temperature setting of 30°C for the conditioner is not suitable for airborne measurement and that the optimal conditioner temperature for low-pressure operation is 27 °C. Under the optimal conditioner temperature (27 °C), the 7 nm cut-off size is also maintained. Additionally, we show that insufficient droplet growth becomes more significant under the low-pressure operation. The counting efficiency of the vWCPC 3789 can vary up to 20% for particles of different chemical compositions (e.g., ammonium sulfate and sucrose particles). However, such variation is independent of pressure.

1 Introduction

Atmospheric aerosol particles are one of the key components of the atmosphere. The currently known ambient aerosol has a size range over several magnitudes and consists of complex chemical compositions, which vary with size, origin, age, and atmospheric processing. This tiny but complicated particulate matter plays a remarkable role in climate change (Seinfeld et al., 2016) and human health (Anderson et al., 2020; Lighty et al., 2000; Pöschl, 2005). To understand the variation of atmospheric aerosol and its production, distribution, and evolution paths, Friedlander introduced a conceptual framework for characterizing instruments used for aerosol measurements (Friedlander, 1970, 1971). Following his framework, the size distribution and number concentration of atmospheric aerosol particles are detected through electrostatic methods and condensational growth. The latter approach is the only technique available for detecting uncharged sub-50 nm particles. Consequently, it has become the dominant technique for assessing the integrated concentration of particles larger than a minimum size.

Since P. J. Coulier and J. Aitken published their observations dealing with the role of a fine airborne particle in the vapor condensation process in 1875 and 1880 separately (Spurny, 2000), the need to understand the phenomena has inspired the development of several particle counting instruments and led to various methods to quantify their performance under different operating conditions (Kangasluoma and Attoui, 2019; McMurry, 2000a; McMurry, 2000b). Several reviews have discussed the

Formatted: Tab stops: 7.06", Left

Deleted: a

Deleted: (wCPCWCPC)

Deleted: has

Deleted: the

Deleted: of wCPC WCPC is

Deleted: .

Deleted: of wCPC WCPC performance

Deleted: low-pressure

Deleted: wCPC

Deleted:

Deleted: variation

Deleted: in the

Deleted: can contribute up to 20% uncertainty in the counting efficiency of the wCPC, but this

Deleted: 100

development of this technique in atmospheric aerosol measurements (Curtius, 2006; Kerminen et al., 2018; Kulmala et al., 2004; McMurry, 2000b). McMurry divided the history of condensation nucleus counters into two main sections through the end of the twentieth century – the development of expansion-type instruments and steady-flow condensation nucleus counters (McMurry, 2000a). Sem describes the designs of three commercial condensation particle counters (CPCs) and characterizes the particle diameter with 50% detection efficiencies of a TSI CPC (3025A, 3022A, and 3010) (Sem, 2002). Two recent comprehensive reviews by Kangasluoma et al. focus on developing instruments that can measure the particle size distribution down to the size of large molecules (Kangasluoma and Attoui, 2019; Kangasluoma et al., 2020). Kangasluoma et al. provide an in-depth review of the effort to advance the technology toward sub-10 nm size distribution measurements, summarize the current understanding of the characteristics of several systems, and identify instrumental limitations and potential advances for accuracy improvement in sub-3 nm particle counting.

In general, an airborne CPC operates by the same principle as standard ground-based CPCs discussed above. It is essential to allow sufficient supersaturation generated inside the condenser for a continuous flow CPC as discussed in this manuscript. Previous studies have described the required modifications of a commercial CPC for aircraft operation and demonstrated how to characterize such sensors under low operating pressures down to 150-200 hPa (Hermann et al., 2005; Hermann and Wiedensohler, 2001; Schröder and Ström, 1997). In the effort to capture the rapid change of the particle concentration from the boundary layer to the stratosphere, the nucleation mode aerosol size spectrometer (NMASS) has been used on research aircraft since 1999. A comprehensive description of the NMASS, its uncertainties under laboratory studies and operation during the Atmospheric Tomography (ATom) mission was published in 2018. Two NMASS were comprised of ten parallel CPCs (five for each NMASS) operating at an internal pressure of 120 hPa. They measured the size distribution between 3 and 60 nm and provided a robust analytical foundation to probe the new particle formation event globally (Brock et al., 2019; Williamson et al., 2018).

Although most CPCs use butanol vapor to grow the aerosol particles, researchers notice that the working fluid plays a critical role in determining the size detection limits, as the vapor properties affect how the vapor condenses upon the particle to enlarge its size for detection. Stolzenburg and McMurry first described the effect of working fluid on size-dependent activation efficiencies with the laminar flow ultrafine condensation particle counter (Stolzenburg and McMurry, 1991), then theoretically described the effect of the working fluid. Experimental studies by Iida et al. (Iida et al., 2009) complemented their theory. Magnusson et al. concluded that working fluids with high surface tension (such as water and glycerol) could lead to a smaller activation size and reduce the lower size detection limit in the CPCs (Magnusson et al., 2003b). For airborne CPCs, 1-butanol and FC-43 (Hermann et al., 2005)are used as a working fluid, and FC-43 shows better performance below 200 hPa. As a working fluid, water avoids the health and safety concerns of butanol or other chemicals. Over the last few decades, mixing type water-based condensation systems have been used to capture particles for online chemical speciation instruments (Khlystov et al., 1995) and high-flow condensation particle counting (Parsons and Mavliev, 2001).

Additionally, water-based CPCs reduce the requirement of chemical storage, maintenance effort, and ventilation system and eliminate water condensation and absorption into alcohol working fluids during operation in humid environments (Liu et al., 2006). However, due to a three times higher mass diffusivity of water compared to butanol, it is very challenging to use water as the condensing fluid in the above thermally, diffusive laminar flow CPC. Therefore, the measurement principle has to be changed (Hering et al., 2005). Hering and Stolzenburg (2005) introduced the concept of a warm, wet-walled condenser for water-based condensational growth. The first implementation of this concept was the two-stage water CPC (Hering et al., 2005). The performance of several versions of this two-stage water-based CPC was intensively evaluated in the 21st century (Biswas et al., 2005; Hakala et al., 2013; Hering et al., 2005; Iida et al., 2008; Keller et al., 2013; Kupc et al., 2013; Kurten et al., 2005; Liu et al., 2006; Mordas et al., 2008; Petaja et al., 2006). In 2014, Hering and co-workers further improved the laminar flow water CPC with

Deleted: in

Deleted: focused

Deleted: To achieve these well-defined conditions, the diffusion of the working fluid in the air should be slower than the heat diffusion.

Deleted: (Hermann and Wiedensohler, 2001; Schröder and Ström, 1997)

Deleted: Over the last few decades, mixing type water-based condensation systems have been used to capture particles for online chemical speciation instruments (Khlystov et al., 1995) and for high-flow condensation particle counting ((Parsons and Mavliev, 2001).

Deleted: ¶
The first laminar flow water-based condensation methods were introduced by…

Deleted: , who

Deleted:

Deleted: her

a third stage to moderate the temperature profile between the growth tube and optics (Hering et al., 2014). This advanced design enables the capture of water vapor by the third moderator stage, such that conditions inside the instrument can be self-sustaining with regard to water consumption under moderate to high relative humidity (Hering et al., 2019; Kangasluoma and Attoui, 2019)). This feature has been commercialized in the "MAGIC" CPC (Moderated Aerosol Growth with Internal water Cycling, ADI). This concept also enables a higher temperature for the second 'initiator' stage, providing supersaturation can be created between the conditioner and initiator, and leads to the activation of 1 nm particles without homogeneous water droplet formation (Hering et al., 2017; Kangasluoma and Attoui, 2019). It further allows flexibility in operating temperatures and a lower detection threshold, and hence has been named the "versatile" water CPC, or vWCPC. The vWCPC has been commercialized by TSI as the Model 3789. Many field deployments confirm that the water-based CPC has comparable performance to a butanol-based CPC in terms of cut-off size and detection efficiency when examining urban pollution and diesel combustion aerosol (Franklin et al., 2010; Jeong and Evans, 2009; Kaminsky et al., 2009; Keller et al., 2013; Lee et al., 2013; Sharma et al., 2011; Tsang et al., 2008). Based on these promising research results, it is desirable to explore the advanced water-based CPC for airborne measurements.

Airborne aerosol measurements provide researchers with *in situ* atmospheric properties across various spatial scales up to thousands of kilometers. However, it also creates design and characterization challenges due to the rapid change in environmental conditions. The pressure dependency of the counting efficiency of non-water-based CPCs has been explored in several studies, and lower cut-off diameter of the CPCs usually increased with the decrease of the operating pressure (Hermann et al., 2005; Hermann and Wiedensohler, 2001; Seifert et al., 2004; Weigel et al., 2009). However, our literature research shows no records about the water-based CPC being evaluated under low-pressure conditions. Thus, this study characterizes a vWCPC 3789 and its counting efficiency changes under such low-pressure conditions. The current simulation was highly nonlinear for the pressures lower than 500 hPa, and the returned solution failed to converge. In addition, we observed inconsistent behavior in one of three vWCPC 3789 we tested. Thus, this manuscript focuses on the measurements and modeling that were done over the pressure range from 500 hPa to 1000 hPa. This pressure range also spans an altitude of 6000 m (~20,000 ft), which is the upper limit for most drone and balloon operations due to FAA restrictions. We examined the 7-nm configuration rather than the 2-nm configuration because the equilibrium water vapor pressure at the maximum temperature in the 2-nm configuration exceeds 500 hPa. A three-stage operating temperature profile simulation was carried out to understand the supersaturation profile inside the water-based condensational growth tube and guide the optimization of the operation setting. A previously developed particle growth model was used to evaluate the pressure change effect on aerosol particle activation and droplet growth. A simplified theoretical analysis is presented to evaluate effects associated with high particle concentrations. Data at low pressures were obtained using a mono-dispersed aerosol of various chemical compositions compared to a CPC operated at atmospheric pressure and a parallel aerosol electrometer at low pressure.

Deleted: (Hering et al., 2017) Kangasluoma and Attoui, 2019)

Deleted: ¶

Deleted: versatile

Deleted: condition

Deleted: d

Deleted: M

Deleted: ed

2 Materials and Methods

2.1 Instrument description and modification

The vWCPC 3789 tested in this study uses a three-stage growth tube, as described by Hering et al. (2017). A single tube with a 6.3mm ID is lined with a wet, porous wick. It has three temperature regions, referred to as the conditioner, initiator, and moderator, with lengths of 73 mm, 30 mm, and 73 mm, respectively. The aerosol flow is 0.3 L/min. The vWCPC 3789 operates in single-particle count mode up to 2×10^5 cm^{-3}. The manufacturer provides two default cut-off diameter settings: 2 nm and 7 nm based on the characteristics by Kangasluoma et al. (Kangasluoma et al., 2017), using particles from a heated tungsten wire in nitrogen flow.

For the 7-nm configuration tested here, the factory default temperature settings of the walls of the conditioner, initiator, and moderator regions are: Tcond=30°C, Tini=59°C, and Tmod=10°C.

Several modifications were made to the unit in this study because commercially available vWCPC 3789 are not designed for low-pressure applications, as shown in Fig. 1. First, the testing vWCPC 3789 was tested to ensure it is vacuum-tight. Therefore, the make-up flow port and exhaust port were blocked during the vacuum-tight check. In addition, the water fill bottle was connected during the vacuum-tight test and low-pressure operations. This step guarantees the instrument operates appropriately under conditions of a significant positive difference between ambient and internal pressures, which mimic the characteristic of the high-altitude operation on an aircraft with a pressurized cabin. Secondly, the vWCPC 3789 monitors the inlet pressure, orifice pressure and nozzle pressure during the operation. Thus, we connected the ambient pressure port and inlet pressure port to the low-pressure manifold, which prevented triggering the warning and error indicator. Thirdly, we added pressure transducers (Baratron 722B, MKS Instruments. Inc., Andover, MA, USA) to the vWCPC 3789 inlet and the exhaust lines. Finally, when we operated with 1.5 lpm inlet aerosol flow, we blocked the make-up flow port. However, we focused on 0.6 lpm inlet aerosol flow in this study. Therefore, when we operated with 0.6 lpm aerosol inlet flow, 0.9 lpm flow from the exhaust line was filtered, passed through a flow buffer, and then made up the 1.5 lpm vacuum flow. Note that under both operating conditions, the aerosol flow passing the condensation tubing and optical particle detector is 0.3 lpm.

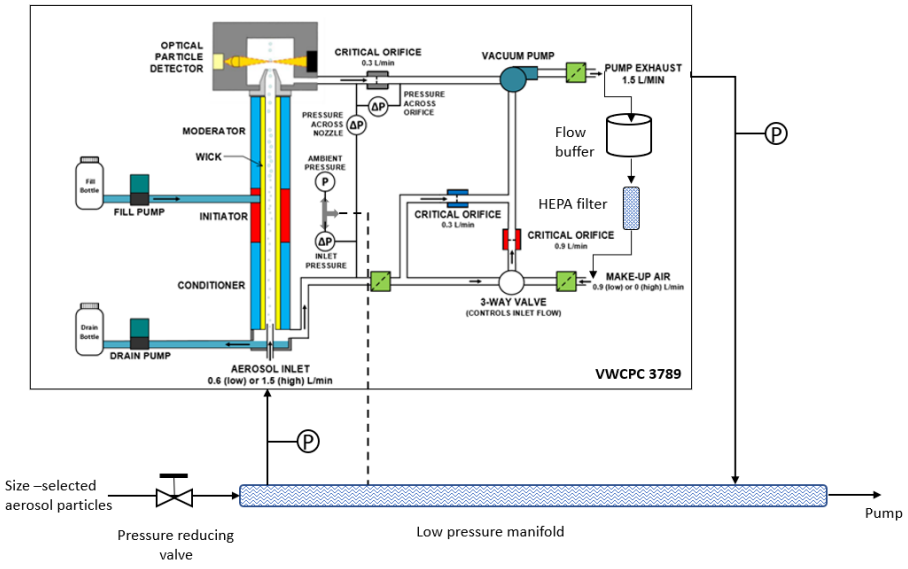

Figure 1: Schematic of the modified vWCPC 3789 sensors and flow system(TSI Incoporated, 2019).

2.2 Experimental characterization setup

The low-pressure calibration setup of the vWCPC 3789 is shown in Fig. 2. Ammonium sulfate was the primary material for this study and was dissolved into deionized water for aerosol generation using atomization techniques. The water-insoluble chemicals, such as humic acid and oleic acid, were atomized from a water suspension after at least 10 minutes of ultrasonic aided mixing. The properties of the other tested aerosol particles were included in Table S1. The tested particles selected in this study were commonly

Deleted: ¶
Deleted: each
Deleted:
Deleted: pressure
Deleted: is monitoring
Deleted: a
Moved (insertion) [4]
Deleted: both
Deleted: in
Deleted: line
Deleted: a pressure transducer (both Baratron 722B, MKS Instruments. Inc., Andover, MA, USA) in
Moved up [4]: (both Baratron 722B, MKS Instruments. Inc., Andover, MA, USA) in
Deleted: W
Deleted: aerosol
Moved (insertion) [1]
Formatted: Indent: First line: 0"

used for the previous CPC characterization (Hering et al., 2014; Hering et al., 2005; Kangasluoma et al., 2017). To increase the aerosol number concentration for particles less than 30 nm, polydisperse ammonium sulfate (AS) aerosols were also passed through a tube furnace generator (Lindberg/Blue, Thermal Scientific, TX, USA) to shift the size distribution a smaller size. Polystyrene latex (PSL) particles were generated through an atomizer. After passing a dilution system, the aerosol particles were size-selected by a differential mobility analyzer (DMA, TSI 3081) using a soft x-ray neutralizer (TSI, advanced aerosol neutralizer 3088). The operating pressure was reduced by a constant pressure inlet (DMT) to simulate different flight level pressures (500 – 1000 hPa). For the counting efficiency determination, two reference sensors were used. One reference sensor was a CPC 3775 (TSI, butanol-based, 50% cut-off diameter is 4 nm), which was connected directly to the monodisperse flow after the DMA and operated at a 0.3 lpm flow rate under the atmospheric pressure. Its inlet aerosol flow rate was 0.3 lpm. The other sensor, an aerosol electrometer (A.E. 3068B, TSI, Shoreview, MN, USA), was operated parallel with the vWCPC 3789 under low-pressure conditions. Both vWCPC 3789 and A.E. were run at 0.6 lpm inlet flow with matched tubing lengths to ensure equal diffusive particle loss in the aerosol pathway. The DMA's sheath flow was typically 20 lpm, resulting in a sheath to aerosol flow ratio and a non-diffusive mobility resolution of 13.

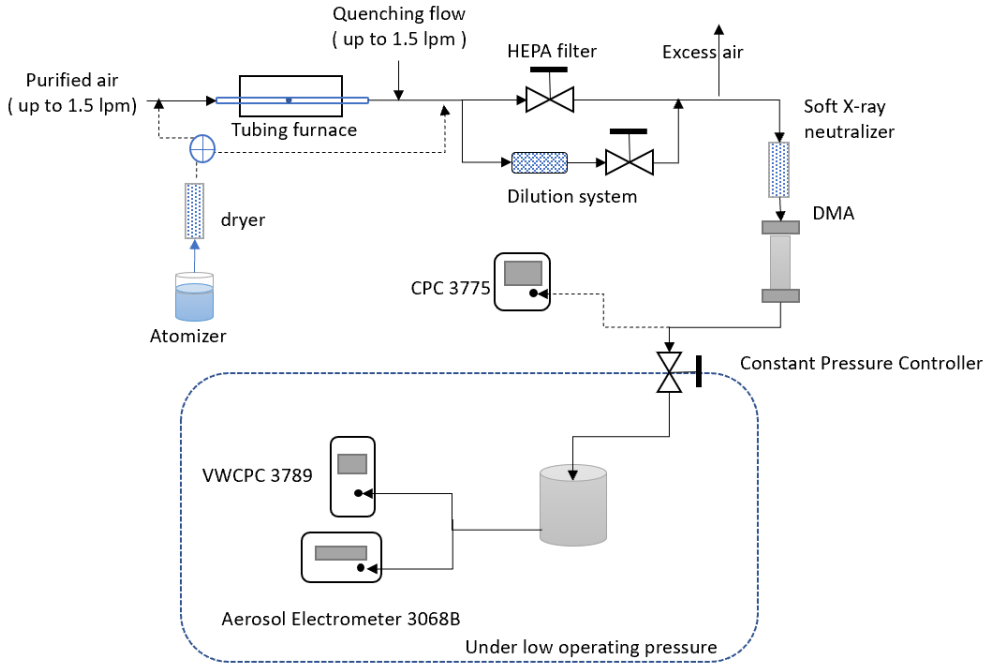

Figure 2. Schematic of the vWCPC 3789 sensors and flow system under the low-pressure testing.

2.3 Numerical simulation

Numerical simulations of the temperature and humidity profiles and the particle growth were calculated for the geometry of the vWCPC 3789 described above, using the methods published by Hering's group (Hering et al., 2014; Lewis and Hering, 2013). The

Deleted: ¶

Deleted: P

Deleted: produced

Deleted: in

Deleted: CPC 3789

Deleted: CPC 3789

Deleted:

Deleted: The CPC counting efficiency is defined by the ratio of the particle number concentration measured by the CPC 3789 and the reference particle number concentration measured by the A.E. Multiple charged particles induce a reading error in the reference particle number concentration. This error is negligible for particle sizes less than 70 nm compared to other experimental errors. (Hermann, 2000; Hermann, 2001). For aerosol particles larger than 70 nm, an empirical correction was estimated using the size distribution of the generated aerosol and the aerosol charging distribution (Tigges, 2015, "Bipolar charge distribution of a soft x-ray diffusion charger") and the particle loss through the constant pressure inlet, which can be estimated based on the total number concentration difference measured by the CPC 3775 and vWCPC 3789.¶ ...

Moved up [1]: Ammonium sulfate was the primary material for this study and was dissolved into deionized water for aerosol generation using atomization techniques. The water-insoluble chemicals, such as humic acid and oleic acid, were atomized from a water suspension after at least 10 minutes of ultrasonic aided

Moved (insertion) [2]

Deleted: 3789

Field Code Changed

assumption and equations used for the simulation are included in the supplemental document. More details are discussed in section 3.2. To summarize the methodology, first, the temperature and humidity profiles were computed using the finite element modeling software - COMSOL Multiphysics® (www.comsol.com. COMSOL AB, Stockholm, Sweden). Next, the particle growth, temperature and humidity profiles were calculated using a numerical model developed by Lewis and Hering (Lewis and Hering, 2013), written in Igor Pro (Wavementrics, Beaverton, OR).

The configuration in Hering's research (Hering et al., 2014) is different from the vWCPC 3789. Hering's WCPC consists of a 4.6 mm I.D. tube extending through a 154 mm conditioner, a 76 mm initiator, and a 100 mm moderator, with a design flow rate of 1.5 L/min. Their simulation results suggest that the three-stage configuration is superior in decreasing the amount of water vapor and lowering the particle loss and variation in detection and collection, avoiding the side-effect of heating the flow. With this "moderated" approach, a short, warm, wet-walled initiator provides sufficient water vapor for activation, followed by a cool-walled moderator for particle growth. A recent simulation study (Bian et al., 2020) confirmed Hering's finding with different temperature settings. In general, enhancing the temperature difference between the initiator and the conditioner can obtain higher supersaturation and smaller activation size.

Furthermore, shifting the 70 °C temperature difference window by decreasing the conditioner temperature (from 9 °C to 1 °C) further reduces the activation size. In addition, Hering's paper pointed out that the final droplet size decreases from around 4.5 µm to 2.5 µm with the increase of the aerosol inlet flow rate from 0.4 lpm to 1.5 lpm. This behavior is consistent with Bian's result, which shows that when the flow rate increased by a factor of 2.5, the final size decreased by 43%.

3 Results and discussion

3.1 Pressure dependence of the vWCPC 3789 counting efficiency

The CPC counting efficiency is defined by the ratio of the particle number concentration measured by the vWCPC 3789 and the reference particle number concentration measured by the A.E. Multiple charged particles induce a reading error in the reference particle number concentration. This error is negligible for particle sizes less than 70 nm compared to other experimental errors. (Hermann, 2000; Hermann, 2001). For aerosol particles larger than 70 nm, an empirical correction was estimated using the size distribution of the generated aerosol and the aerosol charging distribution (Tigges, 2015, "Bipolar charge distribution of a soft x-ray diffusion charger") and the particle loss through the constant pressure inlet, which can be estimated based on the total number concentration difference measured by the CPC 3775 and vWCPC 3789.

Using the low-pressure testing setup shown in Fig. 2, the counting efficiency of a vWCPC 3789 was measured between 500 hPa to 920 hPa for AS particles of 15 nm, 25 nm, and 100 nm (mobility diameter). The aerosol concentrations in this test were maintained in the range $2\sim4\times10^4$ cm^{-3}. The obtained counting efficiencies for the manufacturer's 7 nm cut-off setting are shown in Fig. 3. The conditioner, initiator, and moderator temperatures were 30 °C, 59 °C, and 10 °C under this setting.

During the testing, the temperature variations in the conditioner and moderator were less than ±0.5 °C. For the "7 nm" temperature setting, the initiator temperature has a variation of ±1 °C. The y -axis error bar indicates the standard deviation of the counting efficiency averaged over ~5 minutes of sampling time at a 1 Hz sampling rate. Fig. 3 shows that the counting efficiencies decreased with the decrease of the operating pressure around 700 hPa. The decreases became significant and larger than 10% when the operating pressure was lower than 600 hPa.

Deleted: ¶
The numeric modeling approach used here has been documented in previous publications (Hering et al., 2014; Lewis and Hering, 2013).

Deleted: F

Deleted: The configuration in Hering's research (Hering et al., 2014)consists of a 4.6 mm I.D. tube extending through a 154 mm conditioner, a 76 mm initiator, and a 100 mm moderator, with a design flow rate of 1.5 L/min.

Deleted: ¶

Deleted: .

Deleted: varied

Moved up [2]: Numerical simulations of the temperature and humidity profiles and the particle growth were calculated for the geometry of the vWCPC 3789 described above, using the methods published by Hering's group (Hering et al., 2014; Lewis and Hering, 2013). The assumption and equations used for the simulation are included in the supplemental document. More details are discussed in section 3.2.¶

Deleted: CPC 3789

Deleted: With the 7 nm cut-off size manufacturer setting, the

Deleted: become

Deleted: 500

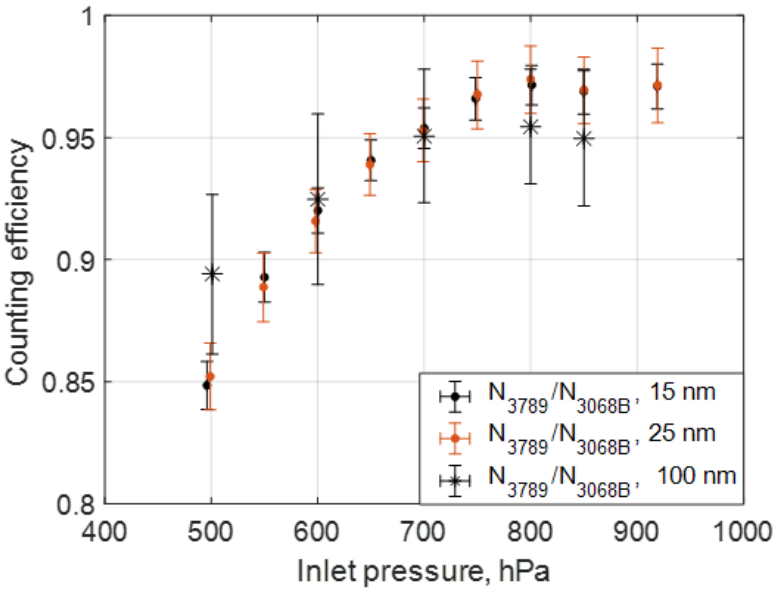

Fig. 3, vWCPC 3789 counting efficiency as a function of the inlet operation pressure at TSI standard conditions: Tcond = 30 °C ,Tini = 59 °C, and Tmod=10°C. N_{3789}/N_{3068B} is the total number concentration ratio between the vWCPC and the electrometer.

Based on the κ-Köhler theory and the supersaturation (relative humidity-1) estimated at the centerline of a three-stage chamber in Fig. S2, ammonium sulfate particles larger than 9.7 nm should all be activated when the saturation ratio is larger than 1.05, even if we assume that the supersaturation profile near the wall has an 85% drop from the centerline condition. Thus, the low counting efficiency under the low-pressure operation condition is not limited by aerosol activation.

Previous simulation studies show that the centerline saturation ratio is not sensitive to the wall temperature of the moderator (Bian et al., 2020; Hering et al., 2014). However, under the low-pressure condition (e.g., 500 hPa), the saturation profile peaked earlier but lower than the saturation profile under the standard condition (1000 hPa), as shown in Fig. S2. Also, decreasing the conditioner temperature (while maintaining the same temperature difference between the initiator and the conditioner) provided higher saturation ratios in the initiator and more water vapor for particle growth, which is also consistent with the previous growth tubing simulation (Bian et al., 2020). Thus, in the following section, we examine the temperature effect on the vWCPC 3789 performance under the low-pressure condition. Furthermore, with the aid of the simulation, we study how to overcome the couniting efficiency decrease experimentally.

3.2 Simulation-aided investigation of the pressure dependence of the vWCPC 3789 counting efficiency at different conditioner temperatures.

Deleted: Modelled
Deleted: study
Deleted: operating
Deleted: condenser

The simulated saturation profiles of a three-stage growth tube at different operation pressure (1000 and 500 hPa) for three different conditioner temperatures (30 °C, 27 °C, and 24 °C), all with initiator temperature of 59°C and moderator temperature of 10°C, are presented in Fig.4. The predicted droplet size evolution along the growth tube of this vWCPC 3789 at different operation pressures (1000 and 500 hPa) under three conditioner temperatures (30 °C, 27 °C, and 24 °C) is included in Fig. 5. In most water-based CPCs,

the aerosol particle growth is initiated by the temperature rise from the conditioner to the initiator. The growth rate is modulated by the temperature decrease from the initiator and the moderator. The maximum saturation ratio calculated at the centerline usually occurs downstream of the initiator exit due to the water vapor diffusion delay. However, in Fig. 4, we observed a double-peaked saturation ratio profile appeared for three different conditioner temperature settings under both operation pressures (1000 and 500 hPa). The maximum saturation peak occurs inside the moderator under most simulated conditions, except when the operation pressure decreases to 500 hPa at the conditioner temperature of 24 °C, the highest saturation peak occurs inside the initiator. Under the standard pressure, this configuration has the advantage that the peak extends close to the wall, resulting in high counting efficiency and a sharp lower cut-off size, as shown in Fig. 5. With the decrease of the operating pressure, the saturation peaks showed a substantial reduction, which was also associated with both the lower cut-off size increasing in Fig. 4. and the growing droplet size decreasing in Fig 5. When the conditioner temperature is 27 °C or 30 °C, with decreasing of the operating pressure from 1000 hPa to 500 hPa, one 8 nm seed particle grew to a smaller size (~40% reduction in the droplet diameter), no matter the particle entered the growth tube in the centerline or near the wall. The seed particles entering the centerline of a growth tube got activated in the initiator. Delay of the activation occurred for the seed particles entering the growth tube away from the centerline, and those particles at 75% of radius started growing in the moderator.

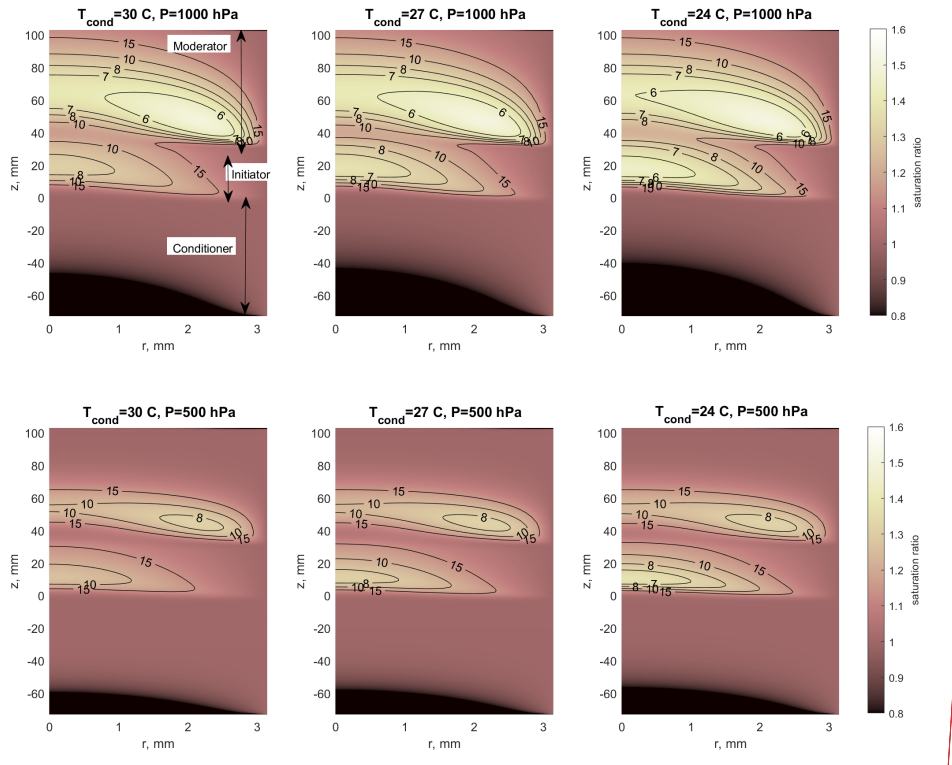

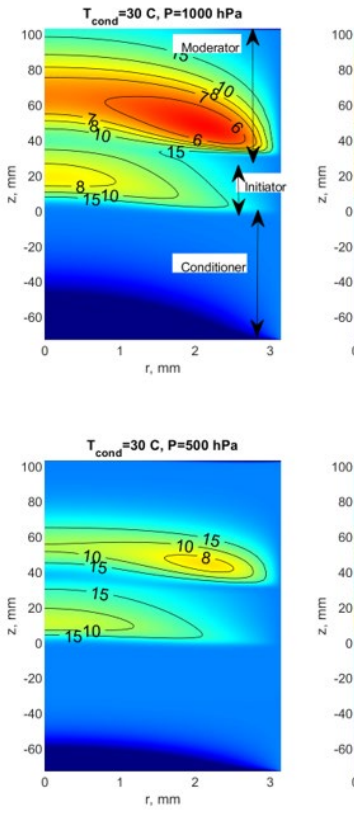

Deleted:

Deleted: was

Deleted: was

Deleted: decreased

Deleted: ,

Fig 4. Simulation of the CPC3789 saturation ratio profiles at 1000 hPa (upper panel) and 500 hPa (bottom panel) under the different conditioner temperatures (30 ℃, 27 ℃, and 24 ℃) with the initiator temperature at 59 ℃, and the moderator temperature is 10 ℃. The color bar indicates the humidity (the saturation ratio) change inside the three-stage growth tube. The contour line indicates the saturation ratio necessary to activate 6, 7, 8, 10, 15 nm seed particles. r is the distance from the centerline. z is the distance from the entrance of the initiator, which means that the conditioner is from -70 to 0 mm.

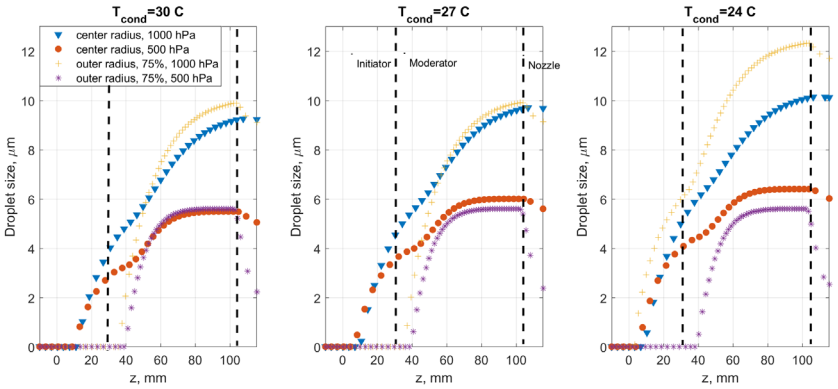

Fig. 5. Predicted droplet size evolution along the growth tube (at centerline or 75% of the inner tubing radius) of the vWCPC 3789 under the different conditioner temperatures (30 ℃, 27 ℃, and 24 ℃) with the initiator temperature at 59 ℃, and the moderator temperature is 10 ℃. Starting particle size 8 nm. The dashed lines indicate the starting and the ending locations of the moderator.

Guided by the above analysis and the observations, we maintained the temperature settings in the initiator at 59°C and moderator at 10°C and varied the conditioner temperatures by 3 ℃. The aerosol particle concentrations for 100 nm size-selected particles were maintained at around $6 \times 10^3 (cm^{-3})$ in this study to avoid the concentration effects (more discussion in section 3.3). Under each conditioner temperature, we examined the impact of the operating pressure on the aerosol particle growth inside the three-stage growth tube through the simulation (shown in Fig. 4, 5, and S2) and on the vWCPC 3789 counting efficiency change through the experiment (as shown in Fig. 6). When the conditioner temperature was set at 30 ℃ or 33 ℃, the counting efficiency drops as the inlet pressure is lowered from 1000 hPa to 500 hPa. However, when the conditioner temperature was decreased to 27 ℃ or 24 ℃, we did not observe a noticeable decrease in the counting efficiency with the operating pressure decrease.

Deleted: is

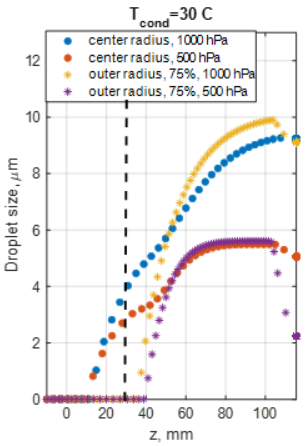

Deleted:

Deleted: is

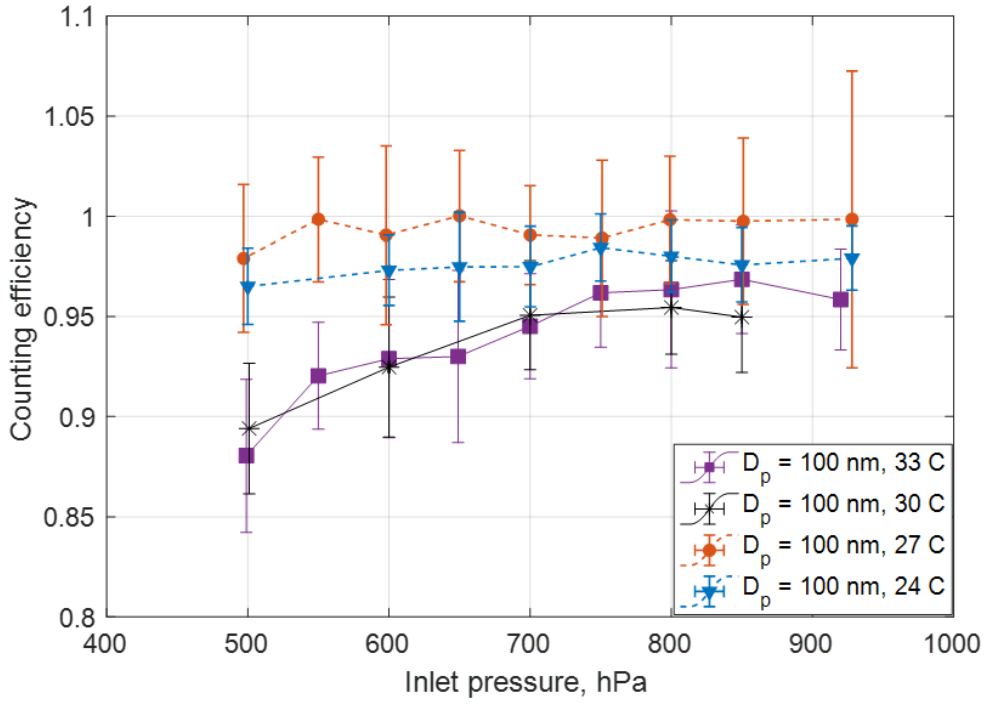

Fig. 6, vWCPC 3789 counting efficiency as a function of the inlet operation pressure at four conditioner temperatures of T_{cond} = 24, 27, 30, 33 °C (Tini=59°C, Tmod=10°C).

Deleted: 3789

The experimental results suggest that increasing the temperature difference between the conditioner and the initiator affected the vWCPC 3789 counting efficiency. As shown in Fig. 6, the counting efficiencies of the T_{cond}=27 °C setting were maintained close to 1 when the operating pressure dropped to 500 hPa. Although we presented data with 100 nm particles in Fig. 6, we observed a similar trend with particles down to 15 nm (Fig. S3). This observation suggests that the low counting efficiency observed in Fig. 3 was not mainly caused by the particle loss inside of the instruments. Fig. 5 suggests that although the 2nd saturation peak in the moderator activated the seed particles and is capable of maintaining droplet growth, about 10% of particles may not grow large enough to be detected in the optical chamber. Therefore, the counting efficiency is more susceptible to the 1st peak of the supersaturation profile in the initiator. In addition, the absolute saturation also set the threshold for successfully operating this vWCPC 3789 under lower pressure. Combining the observations from Fig 6 and Fig S3 and the simulation in Fig. 4 and 5, when the simulated saturation is over 1.3, the counting efficiency maintained close to 1 for aerosol particles larger than 8 nm under low-pressure conditions (500 – 920 hPa). We also noticed that the counting efficiency curve is slightly lower when operating the conditioner at 24 °C than when the conditioner was set to 27 °C. That is possibly due to the high supersaturation profile inside the three-stage tube, leading to larger droplets, especially close to the wall and increased loss at the tubing wall and through the focusing nozzle.

Deleted: imitator

Deleted: 3789

Deleted: 3789

Deleted: 15

3.3 Particle concentration and pressure effects on droplet size and vWCPC 3789 counting efficiency

In typical operation, the manufacturer reports that the single-particle counting concentration is maintained up to a concentration of 2×10^5 (cm^{-3}). The reported "pulse height" by a vWCPC 3789 is not the pulse height value produced by the light scattering signal. It is a calculated parameter, which indicates the fraction of the particle population generating an acceptably high pulse. The manufacturer's manual states that the pulse height is above 0.9 for moderate concentrations (~10-5,000 cm^{-3}). Thus, we examined if this concentration threshold would hold under low-pressure conditions. For 100 nm particles, we observed that the pulse height decreases with the decrease of the operating pressure, as shown in Fig. 7(a). When the operation pressure decreased from 550 hPa to 500 hPa, the pulse height decreased from above 90% to around 80%, as shown in Fig 7 (a). Meanwhile, for 100 nm aerosol particles, the threshold concentration (N_{mea}, under 500 hPa) for a 10% reduction with the pulse height values was about 1×10^4(cm^{-3}), as shown in Fig. 7 (b). When the aerosol concentration was larger than 2×10^4 (cm^{-3}), decreasing the pressure affected the measured aerosol concentration more significantly, as shown in Fig. S6(b). Comparing the pulse height curves, while the conditioner temperature operated at 24 ℃ and 30 ℃, Fig. S6(a) shows that the 30 ℃ case suffered more water vapor shortage while decreasing the operating pressure. Additionally, Fig. S6 shows there is no significant difference between the measured 10% reduction threshold between 20 nm and 100 nm particles when the particle concentration is less than 1×10^4 (cm^{-3}). This observation was consistent with the simulated 10% reduction of s and D_p happened when the $N_{7\mu m} \sim 8.5 \times 10^3$($cm^{-3}$) as discussed in the supplemental material (shown in Fig. S4). Moreover, it indicates that we can monitor the pulse height value to detect the undercounting issue. When the pulse height was less than 80%, the measured aerosol concentration by vWCPC 3789 was about 10% less than the aerosol concentration measured by the electrometer.

Moved down [3]: The pulse height is above 90% for moderate concentrations (~10-5,000 cm^{-3}).
Deleted: is vWCPC uses
Deleted: to
Moved (insertion) [3]
Deleted: describes
Deleted: pulse height is
Deleted: 90%
Deleted:
Deleted:
Deleted: measured
Deleted: threshold (N_{mea}, under 500 hPa)
Deleted: for 100 nm aerosol particles i
Deleted: is
Deleted: S5
Deleted: S5
Deleted: showed
Deleted: there is
Deleted: ,
Deleted: is
Deleted: is
Deleted: simulation estimated
Deleted: shown
Deleted: is
Deleted: is

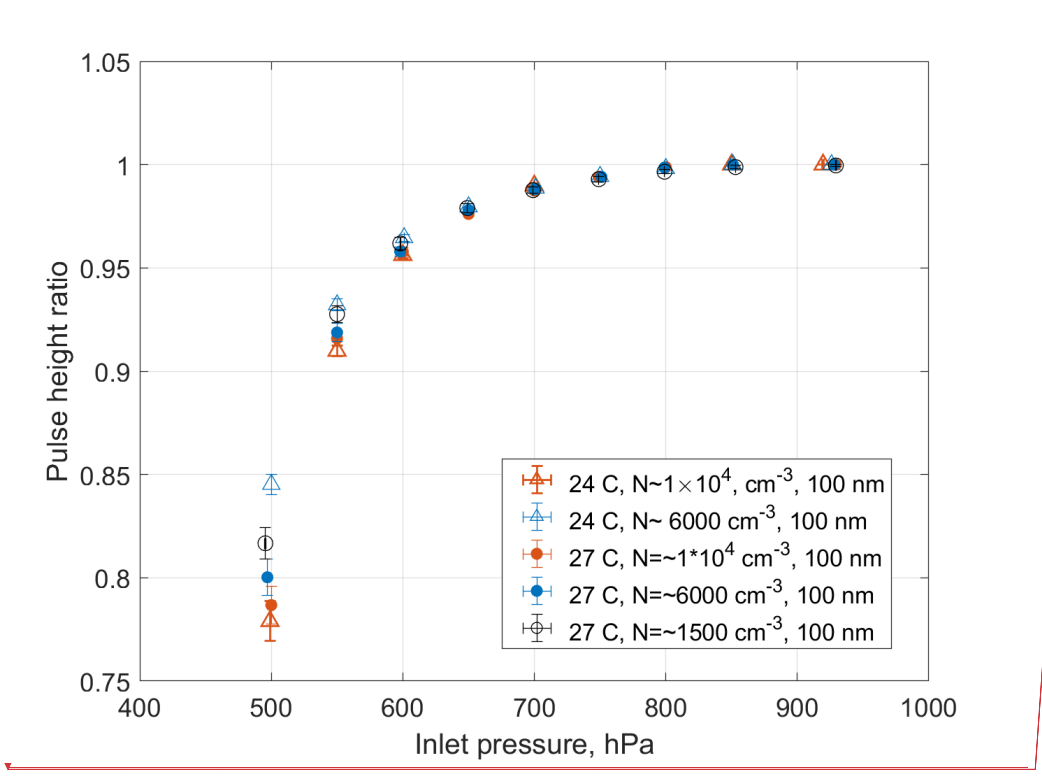
Pulse height ratio
Inlet pressure, hPa
24 C, N~1×10^4, cm^-3, 100 nm
24 C, N~ 6000 cm^-3, 100 nm
27 C, N=~1*10^4 cm^-3, 100 nm
27 C, N=~6000 cm^-3, 100 nm
27 C, N=~1500 cm^-3, 100 nm

(a)

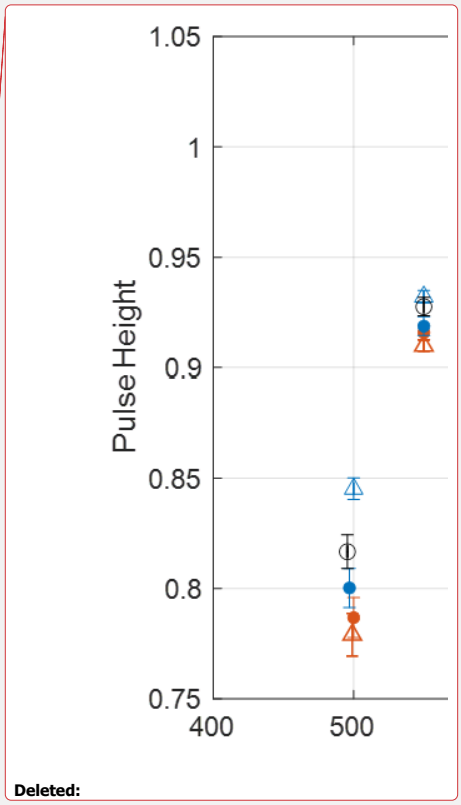
Pulse Height

Deleted:

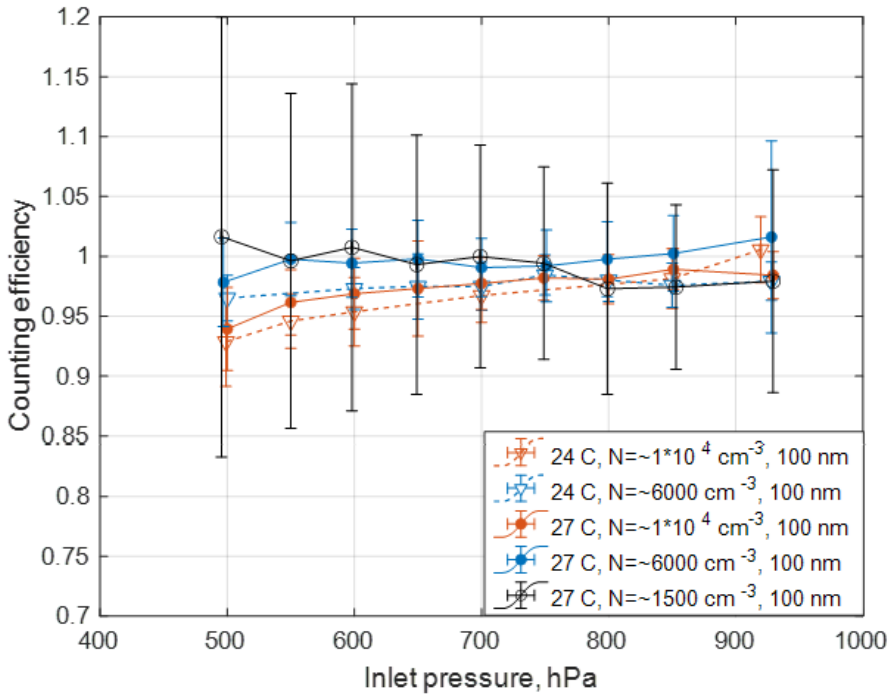

(b)

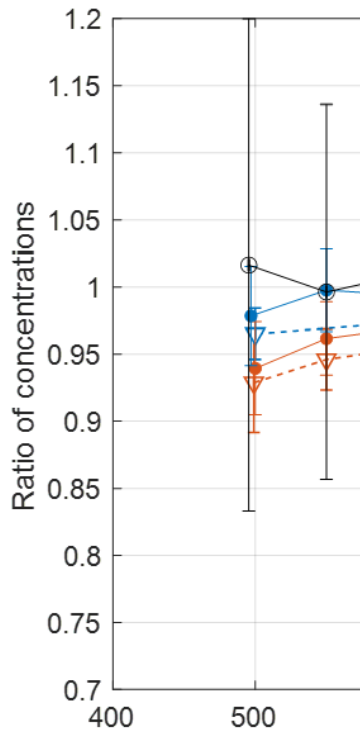

Fig. 7. The water depletion due to the aerosol number concentration, illustrated by (a) the pulse height generated in the optical detector, (b) the counting efficiency as a function of the inlet pressure. Results are shown with the conditioner temperatures set at 24 °C and 27 °C.

3.4 Effect of particle chemical composition on the vWCPC 3789 counting efficiency

We examined the counting efficiency of the vWCPC 3789 using aerosol particles with different chemical compositions and water solubility, as shown in Table S1. During this test, 100 nm aerosol particles were atomized and dried from the ammonium sulfate, sucrose, humic acid and PSL solutions or suspensions before entering the DMA, as shown in Fig. 2. We chose two types of 100 nm aerosol particles: water-insoluble particles, such as oleic acid, humic acid particles and PSL, and highly hydrophilic ammonium sulfate and sucrose particles. Running the 100 nm particles under different operating pressures, we got the counting efficiencies close to 1 for PSL, humic acid and AS particles, as shown in Fig. 8. However, the counting efficiencies of the oleic acid and PSL particles showed more significant uncertainty than that of the ammonium sulfate particles. We could not achieve a reliable curve of the oleic acid particles because oleic acid particles evaporated under low-pressure conditions and caused a significant variation in the number concentration and size distribution of size-selected particles. We noticed that the PSL particle curve has more substantial variation compared to the other aerosol particles. The particle surface is very hydrophobic, and the droplet growth process will be affected by the remaining water or surfactant on the particle surface. The counting efficiency of humic acid particles was slightly lower than the counting efficiency of AS aerosol particles, which could likely be explained by the light-absorbing

Deleted:
Deleted: were
Deleted: ¶
Deleted: Aerosol
Deleted: C
Deleted: effect
Deleted: o
Deleted: three
Deleted: get
Deleted: similar
Deleted: efficacies
Deleted: Therefore, to understand the condensation effect on the droplet size inside the growth tubing, we proceed with a simple analysis to determine the impact. ¶
The chemical composition also affects the observed counting efficiencies. During this test, 100 nm aerosol particles were atomized from the ammonium sulfate, sucrose, humic acid and PSL solutions or suspensions, as shown in Fig. 8. Note that we
Deleted: characterize
Deleted: comparing
Deleted: can

properties of humic acid. The counting efficiency of sucrose is significantly lower than the counting efficiency of AS (10% lower). This observation is consistent with the previous study (Hering et al., 2017). One possible explanation is that the chemical similarity between the seed particle material and the working fluid also affects the detection efficiency of vWCPC 3789 (Wlasits et al., 2020).

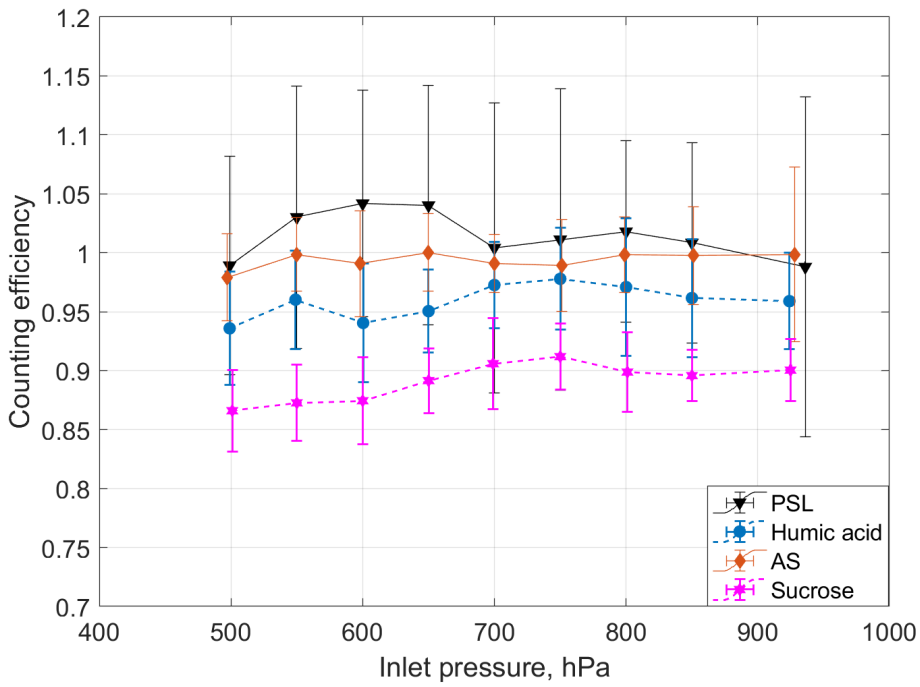

Fig. 8, vWCPC 3789 counting efficiency at different operating pressure with four different types of 100 nm aerosol particles (PSL, humic acid, AS, and sucrose), when the temperature conditions are Tcond = 27 °C and Tini = 59 °C.

3.5 Temperature dependence of the vWCPC 3789 cut-off size

For the butanol-based CPCs, such as TSI CPC 7610, the CPC cut-off size is strongly influenced by the temperature difference between the saturator and condenser (Hermann and Wiedensohler, 2001; Kangasluoma and Attoui, 2019). Typically, the cut-off size decreases with the increase of the temperature difference (Hermann et al., 2005; Hermann and Wiedensohler, 2001). We observed that this trend held well for the vWCPC 3789 using AS particles, as shown in Fig. 9. The temperature effect on the counting efficiency of the vWCPC 3789 under low-pressure conditions is also presented in Fig. 9. With the decrease of the conditioner temperature, the temperature difference between the initiator and the conditioner increases. As expected, the cut-off size slightly moved to lower than 7 nm. However, with the decrease of the operating pressure, the cut-off size increased slightly. Under two conditioner temperatures (24 °C and 27 °C), the cut-off size was maintained between 6-8 nm, even with the pressure dropped to 500 hPa. Thus, both settings are suitable for airborne operations up to 5.5 km with a 7 nm cut-off size. Note that the counting efficiency curve from TSI at 30 °C was derived and fitted using AS particle classified by a custom-made different mobility analyzer (using an aerosol to sheath flowrate ratio of 1:100) under a near-sea-level pressure (Wlasits et al., 2020).

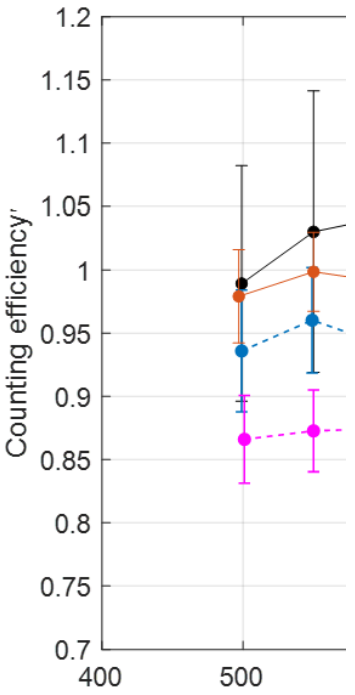

Deleted:

Deleted: was

Deleted: with the increase of the temperature difference, the cut-off size decreases

Deleted: water

Deleted: was

As a result of operation over a much wider pressure range, the cut-off curve derived by this study is less sharp than for the TSI standard settings.

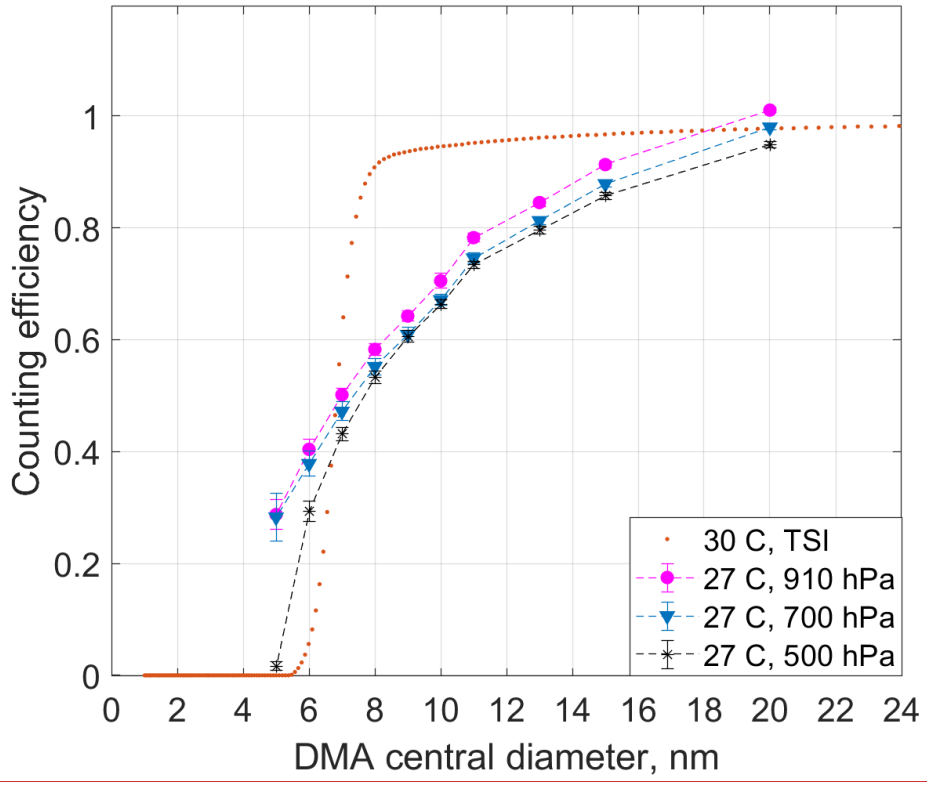

(a)

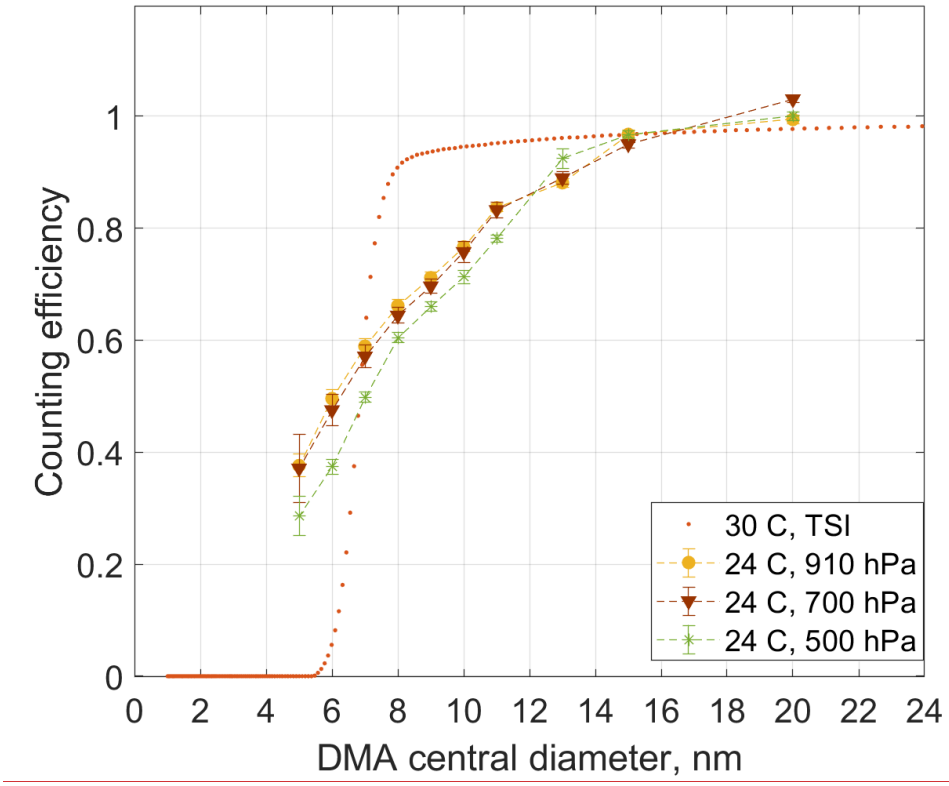

(b)

Fig. 9, vWCPC 3789 counting efficiency changes as a function of the different operating pressures (500, 700, and 910 hPa) using AS particles, when the initiator temperature is 59 °C, and the moderator temperature is 10 °C, at two different conditioner temperatures (a) Tcond = 24, (b) Tcond = 27 °C.

4 Conclusions

This study discusses the modification and characterization of the versatile water CPC (TSI 3789) operating under low-pressure conditions. A commercially available vWCPC 3789 was modified to report the inlet operating pressure during the airborne operation. The vWCPC 3789 counting efficiency was characterized as a function of operating pressure (500 – 920 hPa) for different conditioner temperatures (24 – 33 °C) with the factory settings for the initiator and moderator temperatures (59° and 10°). The vWCPC 3789 with all manufacturer settings (i.e., conditioner temperature of 30 °C) worked as expected under the standard ambient condition (i.e., 1 atm). However, under low-pressure conditions, the counting efficiency of the vWCPC 3789 operated with the factory settings decreased with the decrease of the operating pressure, especially when the operating pressure was below 700 hPa. Although not being able to fully explain the decrease of counting efficiency, numerical simulation and the dimensionless analysis show that the peak saturation ratio at 500 hPa is significantly lower than that at 1000 hPa but occurs closer to the entrance of the

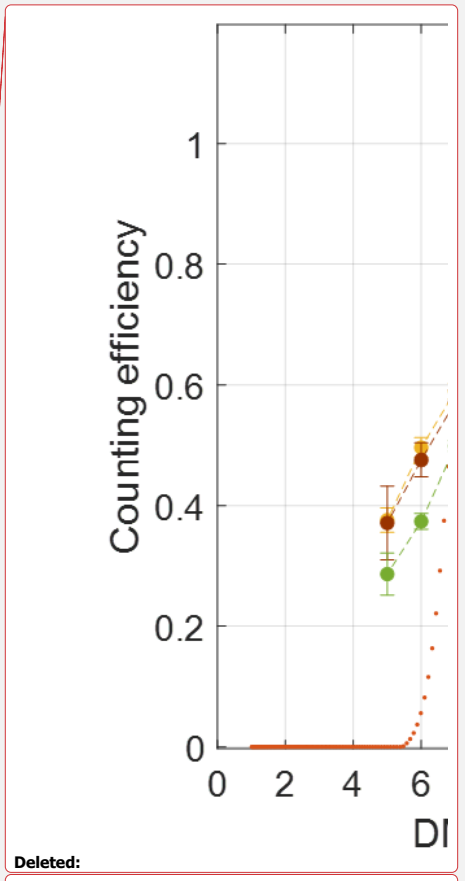

Deleted:

Deleted: ¶

Deleted: environmental

Deleted: A calibration setup was built to study t…he vWCPC 3789 counting efficiency as a function of operating pressure (500 – 920 hPa)…as characterized as a function of operating pressure (500 920 hPa) and…for different conditioner temperatures (24 – 33 °C) with theat…factory settings for the initiator and moderator temperatures (59° and 10°). The vWCPC 3789 with the ...

Deleted: Under

Deleted: we observed that …he counting efficiency of this …he vWCPC 3789 operated at …ith the factory settings decreased with the decrease of the operating pressure, especially when the operating pressure was less than…elow 700 hPa. Although not being able to the numerical simulation with the current assumption could not could not …ully explain the decrease of counting efficiencyis behaviore above phenomena… the …umerical simulation and the dimensionless analysis results …howed…that the peak saturation ratio peak under ...

Deleted: under

Deleted: was …s significantly lower than that e saturation peak ...

Deleted: under

Deleted: arose

initiator. At the same operation pressure, the simulated peak saturation ratio increases with decreasing conditioner temperature. Aided by the simulation results, we examined the effect of conditioner temperature on the counting efficiency and identified an optimal conditioner temperature setting of 27°C for operating the vWCPC 3789 over a range of pressure levels. Additionally, decreasing the conditioner temperature to 27°C did not significantly change the lower cut-off size – 7 nm for the vWCPC 3789. Thus, for the airborne operation down to 500 hPa (~ 6000m above sea level), we recommend operating the vWCPC 3789 with the conditioner temperature setting of 27°C. We also observed that the conditioner temperature has a more pronounced effect on the vWCPC's counting efficiency curve than the operating pressure. A simplified water depletion estimation suggests a 10% reduction of the saturation ratio (s) and the droplet diameter (D_p) under a pressure of 500 hPa when $N_{7\mu m} \sim 8.5 \times 10^3 (cm^{-3})$. The impact of aerosol number concentration on the pulse height reported by the vWCPC 3789 was examined. Similar to the counting efficiency, the pulse height exhibits a decreasing trend with decreasing operating pressure. When the pulse height was larger than 80%, and the particle concentration was less than 1×10^4 (cm^{-3}), a 10% reduction in the measured concentration was observed for 20 nm and 100 nm particles. This observation suggests that the reported pulse height could be used to monitor the potential bias caused by high particle concentration. The chemical composition of aerosol also contributes up to 20% uncertainty in the counting efficiency of CPC, and this uncertainty shows no significant trend with the operating pressure changes when the CPC is operated with the conditioner temperature at 27°C.

The main advantage of vWCPC 3789 is the non-toxic and non-flammable working fluid. Additionally, water has a smaller calculated Kelvin diameter than other working fluids, which means a water-based CPC could lead to a lower size detection limit (Magnusson et al., 2003a). However, for the airborne operation, the elevation will reduce the CPC operating pressure, which limits the highest temperature we could choose for the initiator to push the detection limit lower. Thus, further studies are needed to study how to reduce the lower detection limit of vWCPC 3789 under various ambient pressures.

Acknowledgments: This work has been supported by the Office of Biological and Environmental Research (OBER) of the U.S. Department of Energy (DOE) as part of the Atmospheric Radiation Measurement (ARM) and Atmospheric System Research (ASR) Programs. Battelle operates the Pacific Northwest National Laboratory (PNNL) for the DOE under contract DE-A06-76RLO 1830. We sincerely appreciate the valuable discussion with Andrea Tiwari (TSI), Oliver Bischof (TSI) and Justin Koczak (TSI).

Data availability

The CPC data in the study are available upon reasonable request to Fan Mei (fan.mei@pnnl.gov).

Author contributions

F.M., M.S.P., S.H., and J.W. designed the research. F.M. carried out the measurements. F.M. led the analyses, and S.S. and G.L. led the simulation. F.M. led the writing, with significant input from S.H. and J.W. and further input from all other authors. B.S. and J.T. acquired the financial support for the project leading to this publication. M. H. provided suggestions during the experimental design. S. H., J.W. and B. S. provided suggestions on the revision.

Competing interests

The authors declare that they have no conflict of interest. Susanne Hering and Maynard Havlicek have a commercial interest in the success of the vWCPC instrument.

References

Deleted: Besides, a…t the same operation pressure, with the conditioner temperature decreased, …he simulated peak saturation ratio peaks …ncreases with decreasing conditioner temperatured… Aided by the simulation results, we examined the effect of conditioner temperature effect ...

Deleted: ,

Deleted: . We noticed that setting the …n optimal conditioner temperature setting to …f 27°C was optimal …or operating the vWCPC 3789 under various…ver a range of pressure conditions ...

Deleted: .

Deleted: ¶

Deleted: However, we also observed that the vWCPC's counting efficiency curve varied based on the aerosol total number concentration under higher conditioner temperatures

Deleted:

Deleted: ’

Deleted: up

Deleted: ed

Deleted: al…r temperature setting of 27°C. We also observed that the conditioner temperatures…have… a more pronounced effect on the vWCPC's counting efficiency curve than the operating pressure condition… The … simplified water depletion estimation suggested suggests a that the ...

Deleted:

Deleted:

Deleted: happened when the

Deleted: , while operating at 500 hPa… The impact of aerosol number concentration on We measured …he pulse height reported by the vWCPC 3789 with …as examined. Similar to the counting efficiency, the different aerosol total number concentrations. We. We observed a similar …ulse height exhibits a decreasing trend with decreasing decreasing trend as the counting efficiency when we decreased the ...

Deleted: is

Deleted: 20 nm and 100 nm experienced around

Deleted: particles of

Deleted: ed…that we could use …he instrument's …eported pulse height could be used to monitor the potential bias caused by the ...

Deleted: about

Deleted: there is …his uncertainty shows no significant trend associated …ith the operating pressure changes when the CPC is operateding the ...

Deleted: highly

Formatted: Font: 9 pt, English (United Kingdom)

Formatted: English (United States)

Field Code Changed

Formatted: English (United States)

Anderson, E. L., Turnham, P., Griffin, J. R., and Clarke, C. C.: Consideration of the aerosol transmission for COVID-19 and public health, Risk Analysis, 40, 902-907, 2020.
Bian, J. J., Gui, H. Q., Xie, Z. B., Yu, T. Z., Wei, X. L., Wang, W. Y., and Liu, J. G.: Simulation of three-stage operating temperature for supersaturation water-based condensational growth tube, J Environ Sci, 90, 275-285, 2020.
Biswas, S., Fine, P. M., Geller, M. D., Hering, S. V., and Sioutas, C.: Performance evaluation of a recently developed water-based condensation particle counter, Aerosol Sci Tech, 39, 419-427, 2005.
Brock, C. A., Williamson, C., Kupc, A., Froyd, K. D., Erdesz, F., Wagner, N., Richardson, M., Schwarz, J. P., Gao, R.-S., and Katich, J. M.: Aerosol size distributions during the Atmospheric Tomography Mission (ATom): methods, uncertainties, and data products, Atmos Meas Tech, 12, 3081-3099, 2019.
Curtius, J.: Nucleation of atmospheric aerosol particles, Cr Phys, 7, 1027-1045, 2006.
Franklin, L. M., Bika, A. S., Watts, W. F., and Kittelson, D. B.: Comparison of water and butanol based CPCs for examining diesel combustion aerosols, Aerosol Sci Tech, 44, 629-638, 2010.
Friedlander, S.: The characterization of aerosols distributed with respect to size and chemical composition, J Aerosol Sci, 1, 295-307, 1970.
Friedlander, S.: The characterization of aerosols distributed with respect to size and chemical composition—II. Classification and design of aerosol measuring devices, J Aerosol Sci, 2, 331-340, 1971.
Hakala, J., Manninen, H. E., Petaja, T., and Sipila, M.: Counting efficiency of a TSI environmental particle counter monitor model 3783, Aerosol Sci Tech, 47, 482-487, 2013.
Hering, S. V., Lewis, G. S., Spielman, S. R., and Eiguren-Fernandez, A.: A MAGIC concept for self-sustained, water-based, ultrafine particle counting, Aerosol Sci Tech, 53, 63-72, 2019.
Hering, S. V., Lewis, G. S., Spielman, S. R., Eiguren-Fernandez, A., Kreisberg, N. M., Kuang, C. A., and Attoui, M.: Detection near 1-nm with a laminar-flow, water-based condensation particle counter, Aerosol Sci Tech, 51, 354-362, 2017.
Hering, S. V., Spielman, S. R., and Lewis, G. S.: Moderated, water-based, condensational particle growth in a laminar flow, Aerosol Sci Tech, 48, 401-408, 2014.
Hering, S. V., Stolzenburg, M. R., Quant, F. R., Oberreit, D. R., and Keady, P. B.: A laminar-flow, water-based condensation particle counter (WCPC), Aerosol Sci Tech, 39, 659-672, 2005.
Hermann, M., Adler, S., Caldow, R., Stratmann, F., and Wiedensohler, A.: Pressure-dependent efficiency of a condensation particle counter operated with FC-43 as working fluid, J Aerosol Sci, 36, 1322-1337, 2005.
Hermann, M. and Wiedensohler, A.: Counting efficiency of condensation particle counters at low-pressures with illustrative data from the upper troposphere, J Aerosol Sci, 32, 975-991, 2001.
Iida, K., Stolzenburg, M. R., and McMurry, P. H.: Effect of working fluid on sub-2 nm particle detection with a laminar flow ultrafine condensation particle counter, Aerosol Sci Tech, 43, 81-96, 2009.
Iida, K., Stolzenburg, M. R., McMurry, P. H., Smith, J. N., Quant, F. R., Oberreit, D. R., Keady, P. B., Eiguren-Fernandez, A., Lewis, G. S., Kreisberg, N. M., and Hering, S. V.: An ultrafine, water-based condensation particle counter and its evaluation under field conditions, Aerosol Sci Tech, 42, 862-871, 2008.
Jeong, C. H. and Evans, G. J.: Inter-comparison of a fast mobility particle sizer and a scanning mobility particle sizer incorporating an ultrafine water-based condensation particle counter, Aerosol Sci Tech, 43, 364-373, 2009.
Kaminsky, J. A., Gaskin, E. A. L. M., Matsuda, M., and Miguel, A. H.: In-cabin commuter exposure to ultrafine particles on commuter roads in and around Hong Kong's Tseung Kwan O tunnel, Aerosol Air Qual Res, 9, 353-357, 2009.
Kangasluoma, J. and Attoui, M.: Review of sub-3 nm condensation particle counters, calibrations, and cluster generation methods, Aerosol Sci Tech, 53, 1277-1310, 2019.
Kangasluoma, J., Cai, R. L., Jiang, J. K., Deng, C. J., Stolzenburg, D., Ahonen, L. R., Chan, T., Fu, Y. Y., Kim, C., Laurila, T. M., Zhou, Y., Dada, L., Sulo, J., Flagan, R. C., Kulmala, M., Petaja, T., and Lehtipalo, K.: Overview of measurements and current instrumentation for 1-10 nm aerosol particle number size distributions, J Aerosol Sci, 148, 2020.
Kangasluoma, J., Hering, S., Picard, D., Lewis, G., Enroth, J., Korhonen, F., Kulmala, M., Sellegri, K., Attoui, M., and Petäjä, T.: Characterization of three new condensation particle counters for sub-3 nm particle detection during the Helsinki CPC workshop: the ADI versatile water CPC, TSI 3777 nano enhancer and boosted TSI 3010, Atmos Meas Tech, 10, 2271-2281, 2017.
Keller, A., Tritscher, T., and Burtscher, H.: Performance of water-based CPC 3788 for particles from a propane-flame soot-generator operated with rich fuel/air mixtures, J Aerosol Sci, 60, 67-72, 2013.
Kerminen, V. M., Chen, X. M., Vakkari, V., Petaja, T., Kulmala, M., and Bianchi, F.: Atmospheric new particle formation and growth: review of field observations, Environ Res Lett, 13, 2018.
Khlystov, A., Wyers, G., and Slanina, J.: The steam-jet aerosol collector, Atmos Environ, 29, 2229-2234, 1995.
Kulmala, M., Vehkamaki, H., Petaja, T., Dal Maso, M., Lauri, A., Kerminen, V. M., Birmili, W., and McMurry, P. H.: Formation and growth rates of ultrafine atmospheric particles: a review of observations, J Aerosol Sci, 35, 143-176, 2004.
Kupc, A., Bischof, O., Tritscher, T., Beeston, M., Krinke, T., and Wagner, P. E.: Laboratory characterization of a new nano-water-based CPC 3788 and performance comparison to an ultrafine butanol-based CPC 3776, Aerosol Sci Tech, 47, 183-191, 2013.
Kurten, A., Curtius, J., Nillius, B., and Borrmann, S.: Characterization of an automated, water-based expansion condensation nucleus counter for ultrafine particles, Aerosol Sci Tech, 39, 1174-1183, 2005.
Lee, E. S., Polidori, A., Koch, M., Fine, P. M., Mehadi, A., Hammond, D., Wright, J. N., Miguel, A. H., Ayala, A., and Zhu, Y. F.: Water-based condensation particle counters comparison near a major freeway with significant heavy-duty diesel traffic, Atmos Environ, 68, 151-161, 2013.
Lewis, G. S. and Hering, S. V.: Minimizing concentration effects in water-based, laminar-flow condensation particle counters, Aerosol Sci Tech, 47, 645-654, 2013.
Lighty, J. S., Veranth, J. M., and Sarofim, A. F.: Combustion aerosols: factors governing their size and composition and implications to human health, J Air Waste Manage, 50, 1565-1618, 2000.
Liu, W., Kaufman, S. L., Osmondson, B. L., Sem, G. J., Quant, F. R., and Oberreit, D. R.: Water-based condensation particle counters for environmental monitoring of ultrafine particles, J Air Waste Manage, 56, 444-455, 2006.
Magnusson, L.-E., Koropchak, J. A., Anisimov, M. P., Poznjakovskiy, V. M., and de la Mora, J. F.: Correlations for vapor nucleating critical embryo parameters, J Phys Chem Ref Data, 32, 1387-1410, 2003a.

Magnusson, L. E., Koropchak, J. A., Anisimov, M. P., Poznjakovskiy, V. M., and de la Mora, J. F.: Correlations for vapor nucleating critical embryo parameters, J Phys Chem Ref Data, 32, 1387-1410, 2003b.
McMurry, P. H.: The history of condensation nucleus counters, Aerosol Science & Technology, 33, 297-322, 2000a.
McMurry, P. H.: A review of atmospheric aerosol measurements, Atmos Environ, 34, 1959-1999, 2000b.
Mordas, G., Manninen, H. E., Petaja, T., Aalto, P. P., Hameri, K., and Kulmala, M.: On operation of the ultra-fine water-based CPC TSI3786 and comparison with other TSI models (TSI3776, TSI3772, TSI3025, TSI3010, TSI3007), Aerosol Sci Tech, 42, 152-158, 2008.
Parsons, C. and Mavliev, R.: Design and characterization of a new, water-based, high sample-flow condensation nucleus counter, Aerosol Sci Tech, 34, 309-320, 2001.
Petaja, T., Mordas, G., Manninen, H., Aalto, P. P., Hameri, K., and Kulmala, M.: Detection efficiency of a water-based TSI Condensation Particle Counter 3785, Aerosol Sci Tech, 40, 1090-1097, 2006.
Pöschl, U.: Atmospheric aerosols: composition, transformation, climate and health effects, Angewandte Chemie International Edition, 44, 7520-7540, 2005.
Schröder, F. and Ström, J.: Aircraft measurements of sub micrometer aerosol particles (> 7 nm) in the midlatitude free troposphere and tropopause region, Atmos Res, 44, 333-356, 1997.
Seifert, M., Tiede, R., Schnaiter, M., Linke, C., Mohler, O., Schurath, U., and Strom, J.: Operation and performance of a differential mobility particle sizer and a TSI 3010 condensation particle counter at stratospheric temperatures and pressures, J Aerosol Sci, 35, 981-993, 2004.
Seinfeld, J. H., Bretherton, C., Carslaw, K. S., Coe, H., DeMott, P. J., Dunlea, E. J., Feingold, G., Ghan, S., Guenther, A. B., and Kahn, R.: Improving our fundamental understanding of the role of aerosol− cloud interactions in the climate system, Proceedings of the National Academy of Sciences, 113, 5781-5790, 2016.
Sem, G. J.: Design and performance characteristics of three continuous-flow condensation particle counters: a summary, Atmos Res, 62, 267-294, 2002.
Sharma, N. L., Kuniyal, J. C., Singh, M., Sharma, P., Chand, K., Negi, A. K., Sharma, M., and Thakur, H. K.: Atmospheric ultrafine aerosol number concentration and its correlation with vehicular flow at two sites in the western Himalayan region: Kullu-Manali, India, J Earth Syst Sci, 120, 281-290, 2011.
Spurny, K. R.: Atmospheric condensation nuclei P. J. Coulier 1875 and J. Aitken 1880 (historical review), Aerosol Sci Tech, 32, 243-248, 2000.
Tsang, H., Kwok, R., and Miguel, A. H.: Pedestrian exposure to ultrafine particles in Hong kong under heavy traffic conditions, Aerosol Air Qual Res, 8, 19-27, 2008.
TSI Incoporated: https://tsi.com/products/particle-counters-and-detectors/condensation-particle-counters/versatile-water-based-condensation-particle-counter-3789/, last access: Feb, 2020, 2019.
Weigel, R., Hermann, M., Curtius, J., Voigt, C., Walter, S., Bottger, T., Lepukhov, B., Belyaev, G., and Borrmann, S.: Experimental characterization of the COndensation PArticle counting System for high altitude aircraft-borne application, Atmos Meas Tech, 2, 243-258, 2009.
Williamson, C., Kupc, A., Wilson, J., Gesler, D. W., Reeves, J. M., Erdesz, F., McLaughlin, R., and Brock, C. A.: Fast time response measurements of particle size distributions in the 3–60 nm size range with the nucleation mode aerosol size spectrometer, Atmos. Meas. Tech., 11, 3491-3509, 2018.
Wlasits, P. J., Stolzenburg, D., Tauber, C., Brilke, S., Schmitt, S. H., Winkler, P. M., and Wimmer, D.: Counting on chemistry: laboratory evaluation of seed-material-dependent detection efficiencies of ultrafine condensation particle counters, Atmos Meas Tech, 13, 3787-3798, 2020.

Field Code Changed
Formatted: English (United States)
Formatted: English (United States)

Numerical simulation of three-stage water-based CPC operation

Assumption

1. Water vapor through a cylindrical growth tube is described by the energy equation of a Newtonian fluid under steady laminar flow conditions.
2. The particle flow is assumed to be an incompressible Newtonian fluid with a fully developed parabolic flow profile: $v_z(r) = v_0\left(1-\frac{r^2}{R^2}\right) = v_0(1-x^2)$, where v_0, r, and R represent initial velocity (m/s), radial position (mm), and growth tube radius, respectively, and x is the dimensionless length.
3. Axial thermal diffusion and other second-order effects such as Stefan flow are ignored.

Simplified 1-D heat and mass transfer

The 1-D heat transfer: a partial differential equation of steady laminar flow:

$$v_0\left(1-\frac{r^2}{R^2}\right)\frac{\partial T}{\partial z} = D_{th}\left[\frac{1}{r}\frac{\partial}{\partial r}\left(r\frac{\partial T}{\partial r}\right)+\frac{\partial^2 T}{\partial z^2}\right] \quad (1)$$

D_{th} is the thermal diffusivity of the air, 0.215 cm^2/sec at STP. At the other operation condition in this study, we assume it is constant and the pressure effect is negligible.

The 1-D mass transfer: a partial differential equation for partial vapor pressure:

$$v_0\left(1-\frac{r^2}{R^2}\right)\frac{\partial P_{va}}{\partial z} = D_{va}\left[\frac{1}{r}\frac{\partial}{\partial r}\left(r\frac{\partial P_{va}}{\partial r}\right)+\frac{\partial^2 P_{va}}{\partial z^2}\right] \quad (2)$$

D_{va} is the mass diffusivity of the water vapor, 0.251 cm^2/sec at STP. At the other operation condition, $D_{va,P} = D_{va}/(P/1(atm)) * (\frac{T}{273})^{1.94}$.

Deleted: (0.21 by Steve)

The relative humidity or saturation ratio is defined as the ratio of the partial pressure of water vapor (P_{va}) to the equilibrium saturated vapor pressure of water ($P_{sat,T}$) at a given temperature:

$$S = RH = \frac{P_{va}}{P_{sat,T}} \quad (3)$$

The saturated water vapor pressure can be calculated using Antoine equation (Bridgeman and Aldrich, 1964): $P_{sat,T} = 10^{(A-B/(T+C))}$

A = 5.2039, B = 1733.926, C = -39.485, and T is the temperature in K, and P is the pressure in Pa.

Thus, the above equation can be converted to:

$$v_0\left(1-\frac{r^2}{R^2}\right)\frac{\partial S}{\partial z} = D_{va}\left[\frac{1}{r}\frac{\partial}{\partial r}\left(r\frac{\partial S}{\partial r}\right)+\frac{\partial^2 S}{\partial z^2}\right] \quad (4)$$

Simulation condition

1. The growth tube diameter is 6.3 mm (R=3.15 mm);
2. The conditioner, initiator and moderator tubing lengths are 73 mm, 30 mm, and 73 mm;
3. Inlet conditions: T_0, P_0 is the partial water vapor pressure at T_0.
4. Wall conditions: T_{w1}, T_{w2}, and T_{w3}, and corresponding P_{w1}, P_{w2}, and P_{w3}.

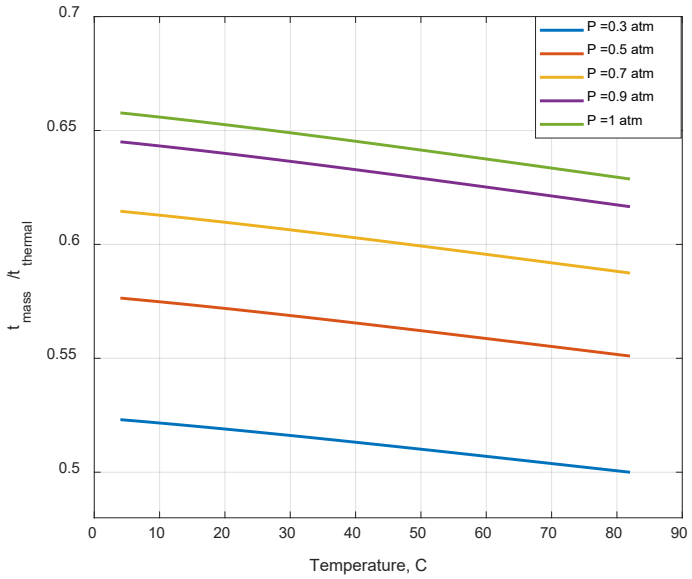

Figure S1. Lewis number as a function of temperature under different operating pressure

Although the configuration of CPC 3789 is different from the previous studies, two fundamental characteristic times can describe how fast the thermal diffusion and the mass diffusion processes will proceed.

$$\tau_{thermal} = \frac{r^2}{D_{th}} = \frac{r^2}{k_a/\rho_a Cp} \quad (5)$$

$$\tau_{mass} = \frac{r^2}{D_{va}} \quad (6)$$

The ratio of those two characteristic times can be designated as the ratio of the thermal diffusivity to the molecular diffusivity of mass, which is also called the Lewis number.

$$Le = \tau_{mass}/\tau_{thermal} = \frac{D_{th}}{D_{va}} = \frac{k_a}{D_{va} \times \rho_a \times Cp} \quad (7)$$

Where r is the radius of the growth tubing, D_{th} is the thermal diffusivity of the air and mainly a function of temperature. D_{va} is the mass diffusivity of the water vapor, which depends on the pressure and temperature, as detailed above. (Seinfeld and Pandis, 2016)

Based on the dimensionless analysis in Fig. S1, with the decrease of the operation pressure, the Lewis number decreases, which means that the difference between the mass transfer rate and the thermal transfer rate increased with the decrease of the operating pressure. Because the current numerical model and theoretical analysis do not predict this observation, if we assume the water depletion and

Deleted: 1

Deleted: 2

Deleted: 3

Deleted: in the supplement

condensational heat release are negligible, two factors most likely contribute to the counting efficiency decreases under the low-pressure condition: the significant loss inside the growth tube (wall effect or through the focusing nozzle) and the insufficient droplet growth inside the three-stage tube.

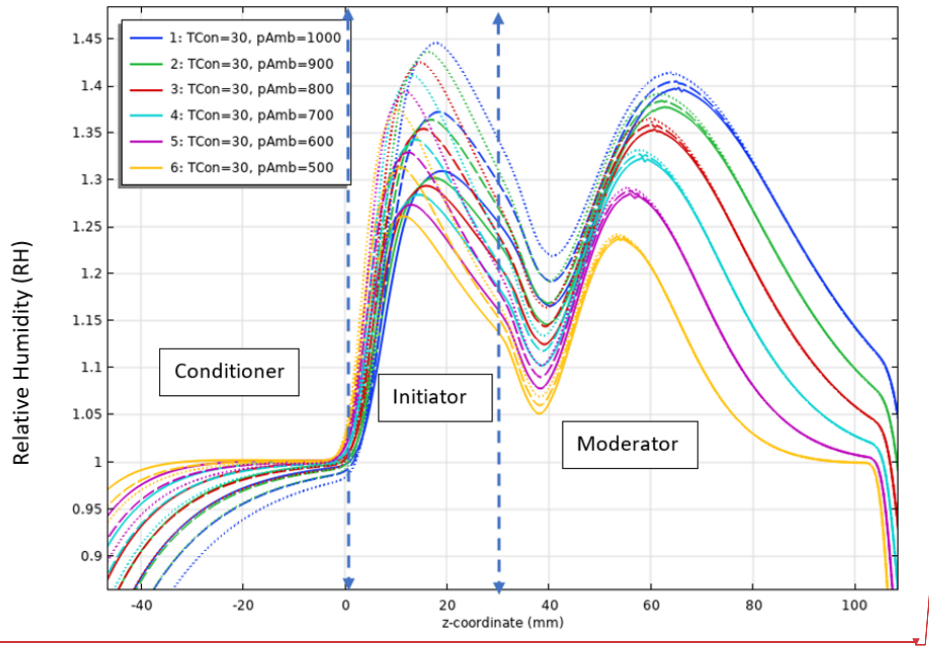

Fig. S2. Saturation ratio calculated along the centerline under different ambient pressures for various conditioner temperatures. The solid lines are for T_{cond} = 30°C. The dashed lines are for T_{cond} = 27°C, and the dotted lines are for T_{cond} = 24°C. The colors indicate pressure in the hPa.

Deleted: *<object>*

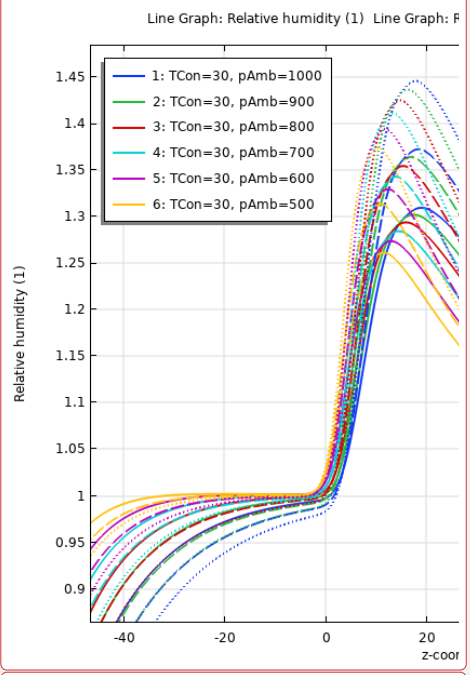

Deleted: at

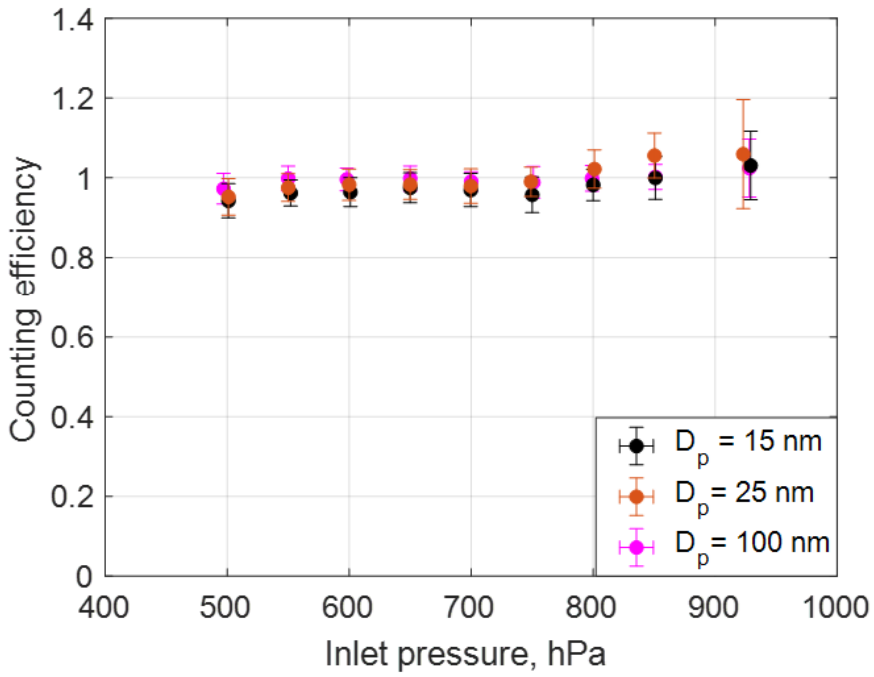

Fig. S3, CPC 3789 counting efficiency as a function of the inlet operation pressure at Tcond = 27 ℃ and Tini = 59 ℃.

Simplified condensation effects on droplet size inside of the initiator

Lathem and Nenes (2011) examined the supersaturation profile generated in a continuous -flow streamwise thermal-gradient growth tubing. Their work shows when water vapor depletion can have an essential impact on supersaturation under certain conditions. The depletion effects on the supersaturation (s) can be described by:

$$s = s_0 - \frac{\pi R^2 R_g T^2}{\Delta H_v G Q P_s} \dot{C} \qquad (8)$$

Where T is the temperature, Q is the aerosol flow rate, R is the radius of the growth tube, P_S is the saturation pressure of the water, and assuming G=dT/dz, and s_0 denotes the maximum supersaturation ratio in the instrument for "zero" particle condition. R_g is the specific gas constant for water vapor. ΔH_v is the enthalpy of evaporation of water, $\dot{C}$ describes the condensational loss (Seinfeld and Pandis, 2016).

The depletion effect leads to a lower supersaturation (s), hence a lower droplet size at the exit of the growth tubing (Nenes and Seinfeld, 2003; Seinfeld and Pandis, 2016).

$$D_p^2 = D_{p0}^2 - 2 \int \Gamma \frac{\pi R^2 R_g T^2}{\Delta H_v G Q P_s} \dot{C}\, dt \qquad (9)$$

Deleted: 4

Deleted: =G

Deleted: the

Deleted: 5

Where D_{p0} is the average droplet size at "zero" particle concentration for $\dot{C} \to 0$.

Γ is a growth parameter that depends on the droplet size and the water vapor mass transfer coefficient (Seinfeld and Pandis, 2016).

$$\Gamma = \frac{1}{\frac{\rho_W R T_\infty}{4 P_{sat,T} D_{va,P}' M_W} + \frac{\Delta H_v \rho_W}{4 k_a' T_\infty}\left(\frac{\Delta H_v M_W}{T_\infty R} - 1\right)} \quad (10)$$

Where k_a' is a modified thermal conductivity described as equation (17.72) by Seitnfeld and Pandis (2016). $D_{va,P}'$ is a modified mass diffusivity described as equation (17.62) by Seitnfeld and Pandis (2016). When calculated the above two modified conductivities, we assume the value of the thermal accommodation coefficient (α_T) was set equal to the mass accommodation coefficient (α_c) in this simplified analysis.

To further simplify the equation (8) and (9), more convenient forms can be derived if $\dot{C}$ is explicitly written as a function of D_p, N, and Γ. The average droplet size $\overline{D_p} = (1/N)\sum_n N_i D_{pi}$.

$$\dot{C} = \frac{\pi R^* T \rho_w}{2 M_w} \Gamma N \overline{D_p} s \quad (11)$$

If we write $\Phi = \frac{\pi^2 R^2 R_g R^* T^3 \rho_w}{\Delta H_v G Q P_s M_w}$, equation (8) can be simplified as

$$\frac{s}{s_0} = \frac{1}{1 + \frac{\Phi}{2}\Gamma N \overline{D_p}} \quad (12)$$

Where R^*, M_w, ρ_w are the universal gas constant (8.314 J/mol/K), the molecular weight and density of liquid water.

The simplification of the droplet size depression equation results from equation (9) and (10)

$$\frac{D_p}{D_{p0}} = \left(1 + \Phi \Gamma N \overline{D_p}\right)^{-1/2} \quad (13)$$

The value of α_c was varied from 1 for rapidly activating aerosol to 0.01 which for slowly activating aerosol. However, based on the estimation, this variation did not significantly affect the saturation and droplet size, as shown in Fig. S4. Additionally, reducing the conditioner temperature also has influenced (<20% with the 15% reduction of s) the saturation profile. Previous studies showed that the droplet size exiting the moderator tube might have up to 90% particle loss if the droplet size is larger than 10 μm (Chen and Pui, 1995; Fletcher et al., 2009; Takegawa and Sakurai, 2011). Meanwhile, the signal-to-noise ratio is too high for small droplets. Thus, this simulation assumed the droplet size exiting the initiator is between 1 to 7 μm.

Deleted:

Deleted: 6

Formatted: Font: Italic

Formatted: Font: Not Italic

Formatted: Font: Not Italic

Deleted: 4

Deleted: 5

Deleted: 7

Deleted: assume

Deleted: 4

Deleted: 8

Deleted: 5

Deleted: 6

Deleted: 9

Deleted: The value of the thermal accommodation coefficient (α_T) is uncertain and was set to equal to the mass accommodation coefficient (α_c) in this simplified analysis. …

Deleted: ,

Deleted: 3

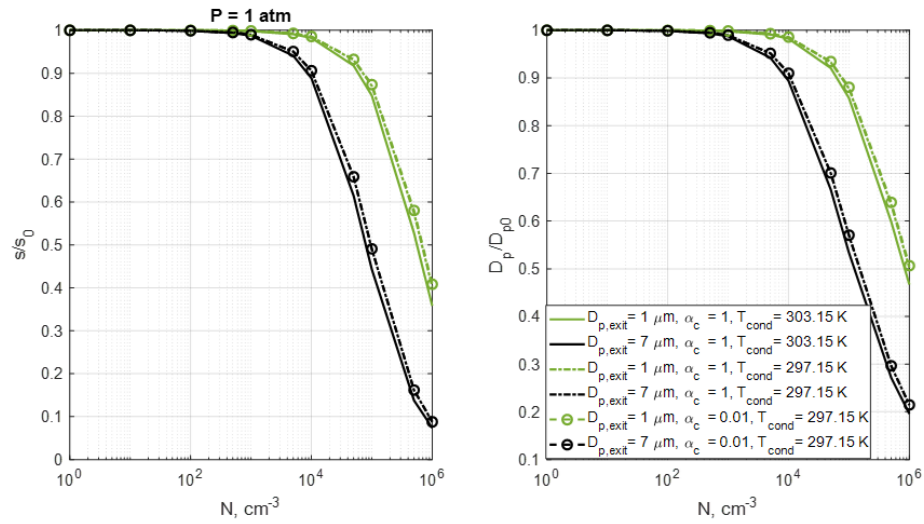

129

130 **Fig. S4. Predicted supersaturation depletion and droplet size depression ratio as a function of aerosol number concentration.**
131 **Results are shown for different mass accommodation coefficients and conditioner temperatures setting.**

132 The wCPC monitors the height of the pulses generated in the optical detector and reports a status
133 parameter to indicate the percentage of the sampled particles, which have an acceptably high pulse.
134 Although the exact droplet size detected by the detector is unknown, this pulse height parameter
135 indirectly shows insufficient particle growth in the detector chamber.

136 The saturation depletion and the droplet size depression are function of the aerosol number
137 concentration at the ambient condition (1 atm), as shown in Fig. S4. The 10% reduction of s and D_p is
138 predicted for $N_{1\mu m} \sim 6 \times 10^4$ (cm^{-3}), the mean droplet size at the initiator's exit is 1 μm with the
139 conditioner temperature setting is 30 ℃. Under the same temperature setting, if the mean droplet size
140 at the exit of the initiator should be 7 μm to make sure the detector counts the particles, the 10%
141 reduction of s and D_p happened when the $N_{7\mu m} \sim 8.5 \times 10^3$($cm^{-3}$). With the conditioner's temperature
142 decreased to 24 ℃, the threshold concentration ($N_{1\mu m}$ and $N_{7\mu m}$) for the 10% reduction of s and D_p
143 increased about 15% ($N_{1\mu m} \sim 7 \times 10^4$ (cm^{-3}) and $N_{7\mu m} \sim 1 \times 10^4$($cm^{-3}$)) from the concentration values
144 under the 30 ℃ conditioner temperature. Thus, the droplet size at the initiator's exit determines the
145 aerosol number concentration limits due to the saturation depletion and the droplet size depression.

146 The simulation results shown in Fig. S4 suggest that the droplet size at the initiator's exit should be
147 larger than 3 μm under the low-pressure. We examined the effect of the operating pressure on the 10%
148 reduction threshold theoretically, as shown in Fig. S5. The theoretical analysis suggests that the 10%
149 reduction threshold ($N_{3\mu m}$) is about 1.94×10^4 (cm^{-3}) at 1 atm, when the conditioner temperature is
150 24 ℃. Based on the theoretical analysis, with the decrease of the operating pressure, the 10% reduction
151 threshold of $N_{3\mu m}$ reduced about 5% of the aerosol concentration (1.85×10^4 (cm^{-3}) at 0.5 atm).

Deleted:

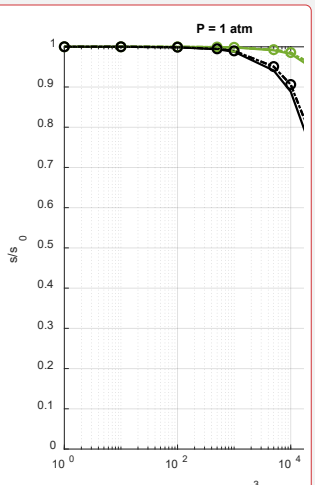

Deleted: setting

Deleted: as

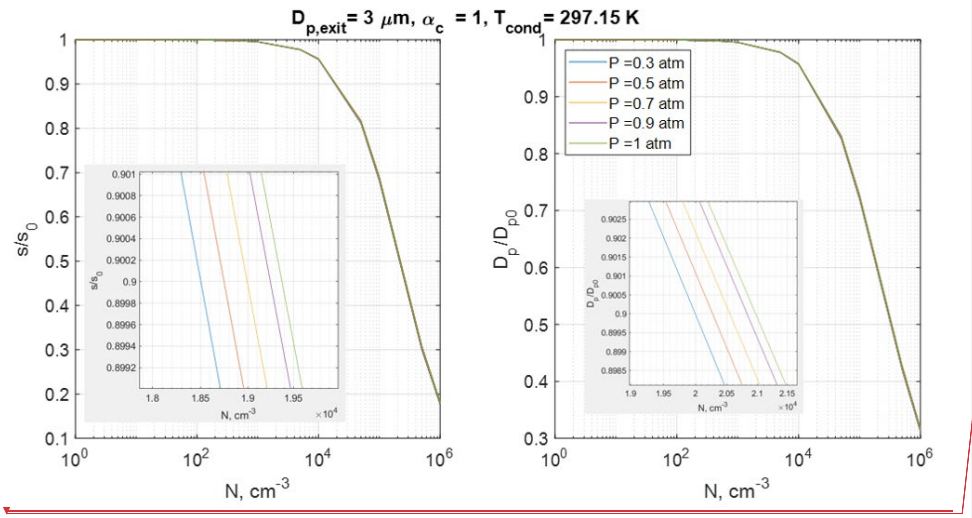

Fig. S5. Predicted supersaturation depletion and droplet size depression ratio as a function of aerosol number concentration. Results are shown for a droplet size of 3 µm exiting the initiator and the conditioner temperature is 24 °C. The insets are zoomed in plots for the narrowed S/S$_0$ range.

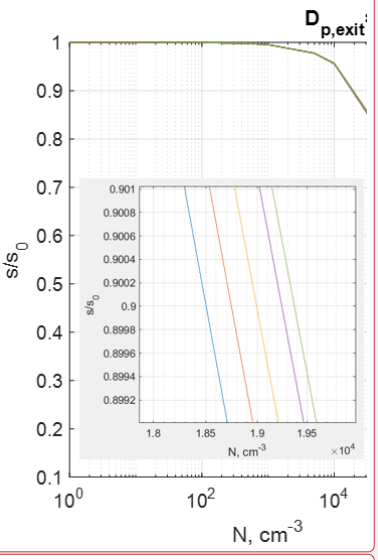

Deleted:

Deleted: the

Deleted: size is

Formatted: Font: Symbol

Deleted: when the droplet

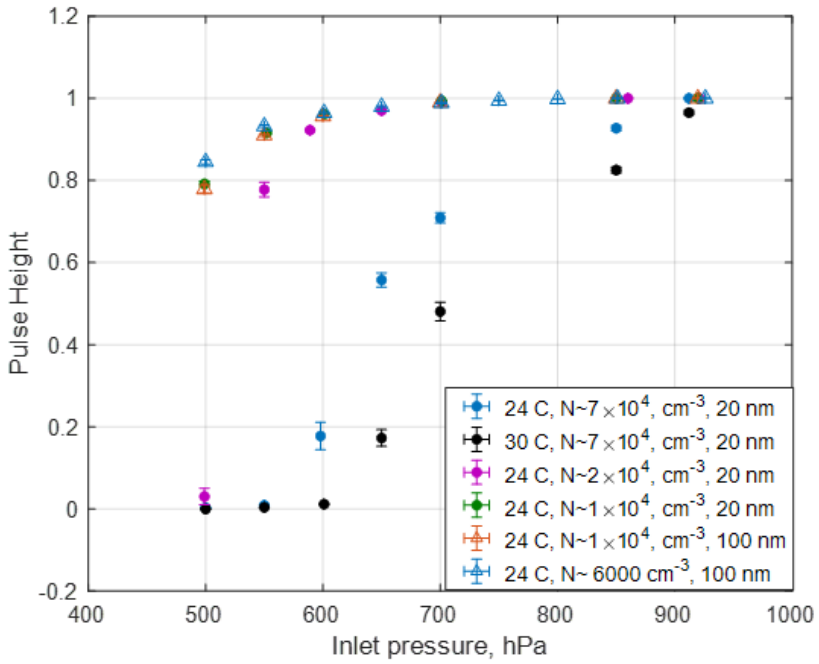
Pulse Height
Inlet pressure, hPa
1.2
1
0.8
0.6
0.4
0.2
0
-0.2
400
500
600
700
800
900
1000
24 C, N~7×10^4, cm^-3, 20 nm
30 C, N~7×10^4, cm^-3, 20 nm
24 C, N~2×10^4, cm^-3, 20 nm
24 C, N~1×10^4, cm^-3, 20 nm
24 C, N~1×10^4, cm^-3, 100 nm
24 C, N~ 6000 cm^-3, 100 nm

(a)

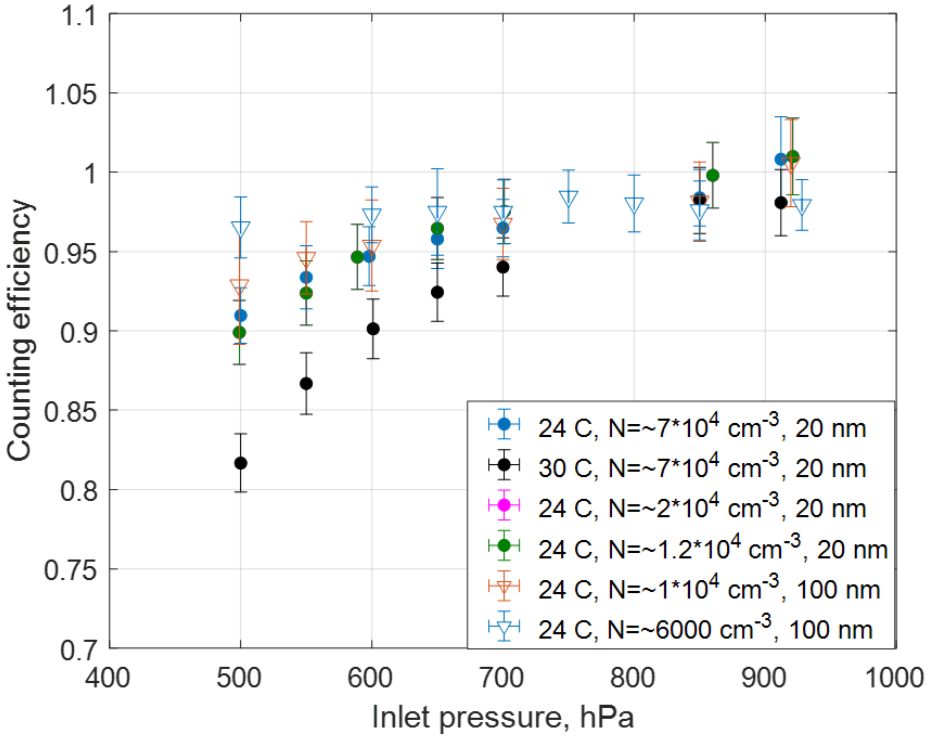

(b)

Fig. S6. The water depletion due to the aerosol number concentration, illustrated by (a) the pulse height generated in the optical detector, (b) the counting efficiency as a function of the inlet pressure. Results are shown with the conditioner temperatures set at 24 °C and 30 °C, with the initiator temperature is 59 ℃ and the moderater temperature is 10 ℃.

Deleted: were

Formatted: Font: 9 pt

Deleted: r

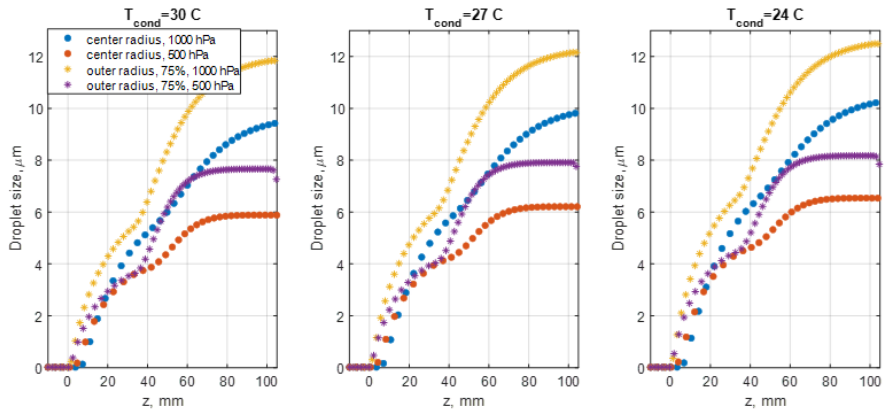

Fig. S7. Predicted droplet size evolution along the growth tube of the CPC 3789 under the different conditioner temperatures (30 ℃, 27 ℃, and 24 ℃), with the initiator temperature at 59 ℃ and the moderater temrperature is 10 ℃. Starting particle size is 20 nm.

Deleted: is

Formatted: Font: 9 pt

Table S1. Properties of tested aerosol particles.

Properties	Ammonium sulfate	PSL	Sucrose	Humic acid	Oleic acid	Water
Molecular weight (g/mol)	132.14	N/A	342.3	227.17	282.47	18.02
Melting point	235 ℃	100-110 ℃*	186 ℃	300 ℃	13.4 ℃	0 ℃
Density (g/cm^3)	1.77	1.055 (20 ℃)	1.59	1.77	0.895	0.997 (20 ℃))
Water solubility	70.6 g/100 g water	insoluble	greater than or equal to 100 mg/mL at 66° F	insoluble	insoluble	N/A
Reference	https://en.wikipedia.org/wiki/Ammonium_sulfate	https://www.thermofisher.com	https://pubchem.ncbi.nlm.nih.gov/compound/Sucrose	https://pubchem.ncbi.nlm.nih.gov/compound/90472028	https://www.britannica.com/science/oleic-acid	https://en.wikipedia.org/wiki/Water

*Glass transition temperature

Formatted: Normal, No bullets or numbering

Reference

Formatted: Left

Bridgeman, O. C. and Aldrich, E. W.: Vapor Pressure Tables for Water, Journal of Heat Transfer, 86, 279-286, 1964.

Chen, D.-R. and Pui, D. Y.: Numerical and experimental studies of particle deposition in a tube with a conical contraction—laminar flow regime, J Aerosol Sci, 26, 563-574, 1995.

Fletcher, R. A., Mulholland, G., Winchester, M., King, R., and Klinedinst, D.: Calibration of a condensation particle counter using a NIST traceable method, Aerosol Sci Tech, 43, 425-441, 2009.

Nenes, A. and Seinfeld, J. H.: Parameterization of cloud droplet formation in global climate models, J Geophys Res-Atmos, 108, 2003.

Seinfeld, J. H. and Pandis, S. N.: Atmospheric chemistry and physics: from air pollution to climate change, John Wiley & Sons, 2016.

Takegawa, N. and Sakurai, H.: Laboratory evaluation of a TSI condensation particle counter (Model 3771) under airborne measurement conditions, Aerosol Sci Tech, 45, 272-283, 2011.